Published on Transportation Research Part C: Emerging Technologies; DOI: 10.1016/j.trc.2025.105069; subject to CC BY-NC-ND license

Tactical Operations of Service Region Dimensioning, Bundling, and Matching for On-Demand Food Delivery Services

Kaihang Zhang[a], Jintao Ke[a, *], Hai Wang[b,c], and Yafeng Yin[d,e]

[a] *Department of Civil Engineering, The University of Hong Kong*
[b] *School of Computing and Information Systems, Singapore Management University*
[c] *Heinz College of Information Systems and Public Policy, Carnegie Mellon University*
[d] *Department of Civil and Environmental Engineering, University of Michigan*
[e] *Department of Industrial and Operations Engineering, University of Michigan*

Abstract

On-demand food delivery (OFD) services have experienced a significant surge in popularity in recent years, which poses various challenges for service operators. To address these challenges, this paper presents an analytical model that captures the complex interplay of the OFD system by considering factors such as adjustable service region size and order bundling. We investigate how key decision variables, namely the maximum delivery distance and bundling ratio, affect the system's endogenous variables and two critical system performance metrics: customer total waiting time and order throughput. Our analysis yields several intriguing managerial insights. First, the maximum delivery distance has a non-monotonic impact on the customer accumulation time, delivery time, and total waiting time, and there is a "win-win" situation in which increasing the maximum delivery distance benefits both the customer total waiting time and order throughput. Second, order bundling is crucial under high customer demand to ensure adequate food delivery supply, but it is less desirable under low customer demand due to increased detour distances in delivery. We further explore strategies for minimizing customer total waiting time (by setting small service regions and bundling ratios) and order throughput (by establishing larger service regions). Recognizing the partial conflict between these two objectives, we identify a Pareto-efficient frontier that serves as a guideline for service operators in balancing these competing goals.

Keywords: food delivery; on-demand services; equilibrium; tactical strategy design

1 Introduction

On-demand food delivery (OFD) service, which allows customers to enjoy take-out meals at home without visiting restaurants in person, has seen substantial growth in recent years. This increase in popularity can be attributed to the widespread use of smartphone technologies and has been further accelerated by the COVID-19 pandemic since people are often reluctant to outdoor activities (Li et

*Corresponding author (kejintao@hku.hk) at: Haking Wong Building F6-05, Department of Civil Engineering, The University of Hong Kong, Hong Kong, China

al., 2020; The Business Research Company, 2023). Many OFD platforms have emerged worldwide to meet continuously increasing OFD demand, such as Uber Eats and DoorDash in the US, Meituan in China, Deliveroo in Europe, and Grab Food in Southeast Asia. These OFD platforms help customers easily locate and order their preferred meals while also providing working opportunities for food delivery drivers (also called couriers). However, as the market expands, these platforms face considerable challenges in efficiently operating the service to accommodate a growing volume of orders. Thus, a comprehensive understanding of the OFD system is crucial for managing such a service, especially in terms of insights into developing effective operating strategies.

The OFD system comprises three entities: merchants (i.e., restaurants; hereinafter, we use the terms "restaurant" and "merchant" interchangeably), customers, and drivers (i.e., meal couriers). Drivers are classified into two statuses, "vacant" and "working". Working drivers are occupied with delivery tasks and vacant drivers remain on standby for task allocation. As a normal practice, the OFD platform dispatches a vacant driver to collectively pick up a bundle of meal orders at a restaurant and deliver them to customers' locations sequentially. The objective of the OFD platform is to manage limited transportation resources (meal couriers) to increase the number of customers who can be served while maintaining or improving service quality, such as by reducing customers' waiting time for meal delivery.

In this study, we examine the tactical strategies employed in the OFD market, considering factors such as adjustable service region sizes, order bundling, and batch-matching processes. Our emphasis lies on the tactical impact of these operations on the market, rather than on long-term strategic goals. Tactical strategy design aims to assess the impact of decisions at a level higher than operational strategies (e.g., real-time driver dispatching), yet not as high as those that consider long-term effects, such as customer and driver dissatisfaction. Two major decision variables are considered: maximum delivery distance R and bundling ratio k. The maximum delivery distance affects the size of the service region for the merchant, with only customers within the area eligible to order from the specific merchant. A smaller maximum delivery distance may exclude some demand and reduce the number of customers served, while a larger distance may accommodate more demand at the cost of longer delivery times. The bundling ratio, which represents the average number of orders in the system that drivers deliver per task, significantly impacts both customer waiting time and driver routing. A larger bundling ratio enables drivers to deliver more orders per trip, thereby increasing the capacity of the food delivery system and potentially allowing the platform to serve more customers. However, bundling more orders per trip may also lead to longer waiting times for customers due to increased delivery duration and the need to accumulate a larger number of orders.

These decisions directly or endogenously impact the entire system and consequently result in a substantial influence on market performance. From the perspective of customers, we consider customer total waiting time to describe customers' experience in the OFD service (from order request to meal delivered). From the OFD platform's perspective, we consider order throughput—the quantity of customer demand that can be served by the system per unit of time. A larger order throughput indicates that the platform has the ability to serve a large number of customers and generate higher profits. However, objectives to improve customer waiting time and order throughput may conflict with each other, and the trade-off must be carefully identified.

We develop an aggregate model to study tactical strategies for the OFD system in a steady-state equilibrium. Regarding the two decision variables discussed in previous paragraphs, it is important to note that they are not directly or homogeneously controlled by the platform in real-world practice. Rather, these decisions may differ across regions and stem from higher-level, specific policies. For

instance, a platform might subsidize drivers to bundle more orders during peak hours to enhance delivery supply or request merchants to expand their delivery areas to serve a greater number of customers. These policies are tailored to address distinct needs and are ultimately reflected in changes to decision factors. Consequently, to streamline our analysis in this study, we concentrate on the tangible manifestations of operations, treating the maximum delivery distance and bundling ratio as decision variables. This approach assumes that these variables can be manipulated through specific, high-level operations. Despite the potential weakness of our simplification, this approach allows us to provide an analytical framework for examining intricate operations related to service region size and bundling strategy. Our proposed modeling framework incorporates a batch-matching mechanism (we use τ to represent the matching time interval) that considers order bundling within a specific service region. We use the continuum approximation (CA) technique to approximate pickup/delivery route length and leverage its advantage to study the impact of maximum delivery distance and bundling strategy on the system performance. The paper's major contributions are as follows.

1. We clearly define an analytic framework for the OFD market and figure out four scenarios of the OFD market based on supply–demand relationships using two criteria. The first criterion concerns the relationship between supply and demand—specifically, whether the market is demand-dominant or supply-dominant. This is determined by whether the number of accumulated order bundles is greater than the number of vacant drivers (demand-dominant) or not (supply-dominant). The second criterion involves whether drivers have to wait at the restaurant for meal pickups, since drivers may arrive at the restaurant before the meals are prepared and ready for pickup.

2. We study the equilibrium states of an OFD market under each market scenario. Our model provides closed-form solutions for important endogenous variables, such as customer total waiting time, customers' delivery time, and more (see Table 1).

3. Our analysis offers managerial insights, including but not limited to, (a) maximum delivery distance has a non-monotonic effect on customer accumulation time, delivery time, and total waiting time, and there exists a win-win scenario in which increasing maximum delivery distance can benefit both customer waiting time and order throughput; (b) a larger bundling ratio benefits the system by increasing the average number of orders a driver could serve in a trip, but it hurts the system by prolonging customers' waiting time. We find that the order bundling strategy is favored in circumstances with higher customer demand, but it is not desirable for the system when demand is low.

4. We investigate optimal tactical strategies aimed at optimizing either customer waiting time (reflecting customer satisfaction) or order throughput (reflecting the market scale). We also derive the Pareto-efficient frontier, which aligns the two objectives by solving a bi-objective optimization problem. This enables us to pinpoint the trade-offs between providing high-quality service and maximizing the market size.

The rest of the paper is organized as follows. Section 2 provides a literature review of related work and discusses a gap in the research. Section 3 presents details of the model and analysis. Section 4 presents a closed-form solution for the OFD system and model properties. Section 5 discusses tactical strategies under two objectives. Section 6 describes a set of numerical experiments and validates the properties and insights, and Section 7 concludes. All proofs are contained in the Appendices.

2 Literature review

OFD services belong to a category called transportation-enabled services (see Wang (2022) and Agatz et al. (2024)) which includes many sub-services such as ride-sourcing (see Wang and Yang (2019)) and on-demand vehicle-sharing services (e.g., Benjaafar et al. (2022)), among others. Different methodologies are applied for supply–demand management and we classify the literature into three categories, namely data-driven approaches, network analysis, and aggregate modeling analysis.

The first cluster of research utilizes the availability of OFD datasets and derives policy implications. For example, empirical analyses including Mao et al. (2019) on customer behavior, Liang et al. (2024) on merchant behavior, and Nguyen-Phuoc et al. (2022) on driver behavior provide valuable insights into the OFD market. Alternatively, machine learning–based methods are also popular to conduct demand analysis. Zhu et al. (2020) estimate order-fulfillment cycle time using a deep neural network, and Liang et al. (2023) predict the demand range in OFD using a Poisson-based distribution prediction approach. The second stream of studies focuses on optimization models and the allocation of resources at a network level, such as routing problems for pickup and delivery (Yildiz and Savelsbergh, 2019b; Reyes et al., 2018) and order assignment problems (Liu et al., 2021; Ye et al., 2024a). Since the optimization problem is usually NP-hard, acceleration in the problem-solving process is essential. Some of these optimization frameworks are data-driven, e.g., Yang et al. (2024) and Behrendt et al. (2023), while some use heuristics to solve the problem efficiently (e.g., Simoni and Winkenbach (2023)). These works focus on problems in short-term operations such that the methods can be readily implemented in real practice while they are typically problem-oriented thus lacking of high-level interpretation of the market, which is another direction of the literature. The third stream develops analytical models for the behavior of customers, drivers, and restaurants and their endogenous interactions. This paper falls into this category. These models can provide managerial insights for OFD platform operators. Some arguments are regarding the downside of online platforms to the market. For instance, Baron et al. (2023) find that the online ordering option for traditional brick-and-mortar stores may hurt both customers' individual utility and social welfare which is discussed by Chen et al. (2022) as well. Others argue the benefits of OFD services and the ways to improve the service level (e.g., Bahrami et al. (2023); Ye et al. (2024b)). The intricate discussions surrounding these conflicts highlight the complexity inherent in the OFD market, thereby necessitating a deeper and more comprehensive understanding of this particular market. These works analyze the system from a high-level perspective and usually adopt approximation methods (see Wang and Odoni (2016), Zha et al. (2018), etc.) or economic analysis (see Yang and Yang (2011), Zhou et al. (2022), etc.) to study the average behavior of the system, and ultimately draw managerial insights into operations.

Motivated by the challenges of the platform operation of OFD, it is important to understand the service system from a high-level perspective. Tactical design problem including fleet sizing and service region design plays an important role. Yildiz and Savelsbergh (2019a) are the first, to the best of the authors' knowledge, to develop a single-restaurant model and find insights into the impact of the service region on profit. Bahrami et al. (2023) construct a strategy for designing the pricing and staffing problems and examine the interactions between the three parties (customers, merchants, and drivers). Ye et al. (2024b) develop a physical model on matching and delivery and study the market demand-supply equilibrium within an optimization framework from an aggregate perspective. Their work provides managerial insights into OFD operations in bundling and pricing strategies. Ke et al. (2024) develop a model to characterize the equilibrium of the OFD system and provide strategies for various market scenarios. Drawing on real-world data, they argue that drivers

might spend extra time for drivers after arriving at the merchant, which contradicts assumptions in previous studies.

Prior studies have addressed several problems, but few have focused on optimizing key tactical decision variables. Moreover, some essential characteristics of OFD markets have not been thoroughly explored. First, the joint consideration of order bundling and service region sizing has not been well studied from a high-level perspective, nor has it had an impact on the interactions with other market players. Second, most studies primarily concentrate on monetary variables, such as driver commissions and delivery fees without paying adequate attention to critical tactical decisions together such as maximum delivery distance and bundling ratio. Our study aims to fill this gap in the research by developing an analytical model to describe the equilibrium of an OFD market and the complex relationships between the system's endogenous variables and the platform's decisions. The model considers the tactical operation, in which the operation strategies have an impact on the OFD system, but do not yet lead to long-term effects such as customer dissatisfaction. Our model outlines the market-clearing conditions under which the customer arrival rate equals the idle driver arrival rate, as well as the transitions of drivers among idle, pickup, and delivery statuses. Specifically, we examine the impacts of two decision variables (maximum delivery radius and bundling ratio) on system performance and offer managerial insights. Furthermore, we analyze optimal tactical strategies for customer total waiting time and/or order throughput and identify the Pareto-efficient curve on bi-objective operations.

3 Model

This section provides the details of our model for the OFD system in an equilibrium state. Notation is summarized in Table 1.

3.1 How the on-demand food delivery system works

The OFD system is composed of three market players, i.e., customers, drivers, and merchants. On top of them, there is a central platform having the decision power to influence the market such as matching and driver assignment (in some markets, there are multiple platforms competing with each other but in this study, we treat the platform as one player). In reality, the platform normally dispatches customer orders to drivers dynamically based on real-time delivery supply and demand situations and uses some carefully designed metrics depending on driver proximity, on-time performance, and drivers' behavior, among others. According to a recent report by a Chinese leading OFD company Meituan (Zhao et al., 2024), the platform also holds the flexibility to postpone the order assignment to seek a better matching result, interpreted as batch matching, and its benefit is amplified by the bundling delivery strategy.

In this study, we study the OFD system at an aggregate level, which means we attempt to build a stylized model to represent the most important features of the market regarding our research focus but maintain the simplest possible model structure. Also, we study the average behavior of market players and analyze the high-level insights into the impact of decision variables which are the maximum delivery distance R and the bundling ratio k. We consider a market where there are multiple restaurants distributed across a region and customers who are interested in ordering food from some restaurant are spread around each of them. The platform allows customers within a fixed delivery region within the maximum delivery distance to order food from the merchant. The distribution of customers in the space should follow certain distributions that

Table 1: Notation

Notation	Description
Exogenous variables	
M	Number of merchants in the area studied
N	Total number of drivers (vehicle fleet size)
v	Average speed of drivers
δ	Customer demand density rate
η	Coefficient to calibrate the return-pickup route length
τ	Matching interval
τ_M	Merchant's average meal preparation time for one order
Decision variables	
k	Bundling ratio, number of orders per delivery batch
R	Maximum delivery distance
System metrics	
W_c	Customer total waiting time
q_t	Order throughput of the OFD system
Waiting times	
$W_{c,a}$	Customer waiting time for order accumulation for a bundle
$W_{c,d}$	Customer average delivery time
$W_{c,q}$	Customer expected waiting time for matching
W_{fp}	Waiting time due to food preparation
W_p	Return-pickup time for drivers
W_v	Driver total time of being vacant and working statuses
$W_{v,d}$	Driver total delivery time in a trip
$W_{v,q}$	Driver expected waiting time for matching
Intermediate variables	
q	Realized order arrival rate from customers
λ	Arrival rate of vacant drivers
λ_0	Matching rate between drivers and order bundles
N_b	Number of order bundles at the end of the matching interval (before next matching decision)
N_s	Number of awaiting drivers at the restaurant for meal preparation at the end of the matching interval (before next matching decision)
N_v	Number of vacant drivers at the end of the matching interval (before next matching decision)
N_w	Number of working drivers at the end of each matching interval (before next matching decision)
L_d	Driver approximated delivery distance
L_a	Driver approximated axial travel distance of delivery
L_p	Driver approximated return-pickup distance
L_t	Driver approximated transversal travel distance when delivering
p_c	Matching probability of order bundles
p_v	Matching probability of drivers
r	Distance from customer to merchant
θ	Angle of the half-sector of each delivery driver's delivery area

can be extracted from real-world data or be predetermined as a priori. We will show in the next subsection how to mathematically formulate the customer demand. Although we assume a uniform distribution of customers in the analysis of model properties, we leave a general illustration in the model introduction and formulation. On the other hand, drivers are considered to follow an approximated routing behavior, and in this study, we use the continuum approximation method to describe drivers' delivery routing.

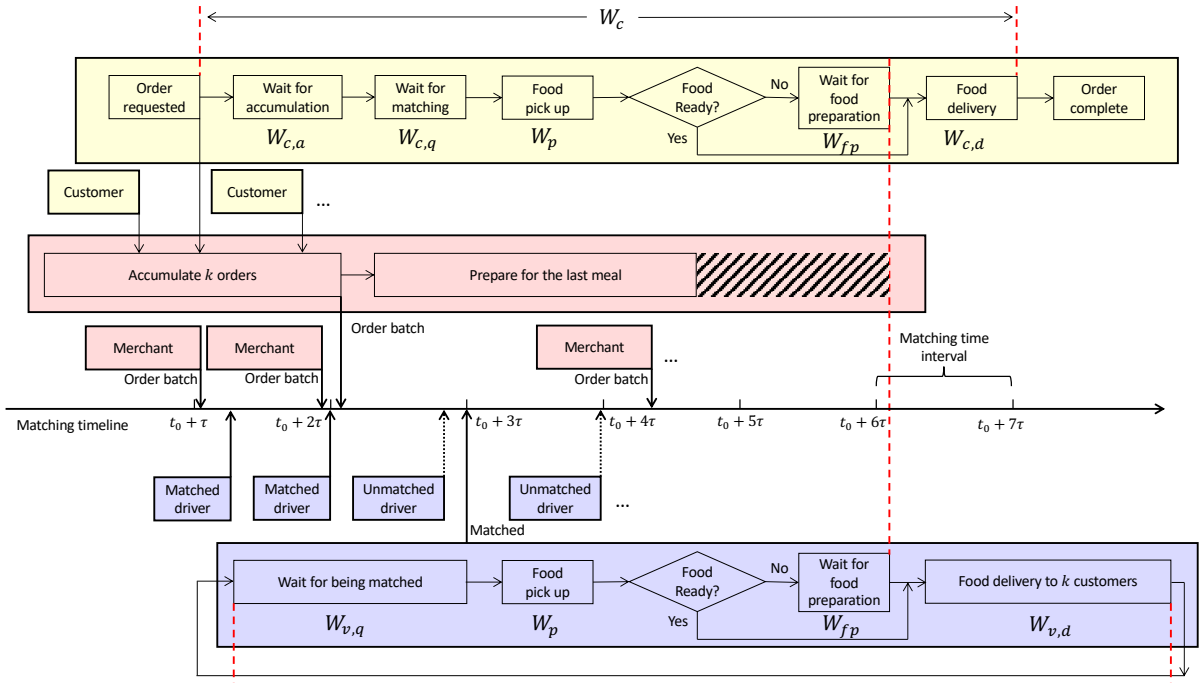

Figure 1: Flow of the on-demand food delivery system. Yellow bars represent customers who choose the merchant for OFD service. Red bars represent merchants who submit batches of orders. Blue bars represent drivers.

The OFD system in this study is based on a batch-matching process that happens every τ amount of time (the matching time interval), which means that the matching is not instantaneously happening every moment but periodically. Although subsequent analysis reveals that the matching interval should be set small, we leave it into the model for completeness and interpretability. Having this postponing matching normally provides better matching results (Yang et al., 2020) with a sacrifice of minor waiting time (i.e., the matching interval). Some other postponing behaviors such as delaying a bundle to another matching cycle (e.g., see Zhao et al. (2024)) is not considered in this study. This batch-matching base setting has been adopted by other on-demand services (e.g., Yang et al. (2020); Li et al. (2024)) and it is also used by some major OFD service providers, such as Meituan (Zhao et al., 2024).

Figure 1 describes the three parties of the OFD system—i.e., customers (yellow), merchants (red), and drivers (blue)—interacting with each other as coordinated by a centralized platform. We use the horizontal axis to represent time. Customers first request an order using their personal devices, and merchants immediately start to prepare the meal upon receiving the order. Each customer may wait for a certain time (denoted by $W_{c,a}$) until the merchant accumulates a bundle of k orders for a bundled delivery. After the merchant accumulates k orders, the orders are bundled as a batch and are ready to be dispatched by the platform to a driver. The accumulation process is a unique characteristic of OFD services because of order bundling. The order accumulation allows the platform to have multiple orders consolidated as a bundle. It is worth noting that the order accumulation process happens before matching, during which drivers are assigned an entire bundle containing several orders. The matching process—i.e., of order bundles and vacant drivers—is performed pair by pair and executed at the end of each matching time interval. Customers are

subject to $W_{c,q}$ amount of the waiting to be matched. After order bundles are matched to vacant drivers, drivers may spend W_p amount of time heading to pick up the meal. When drivers arrive at the merchants, there exist two scenarios: the merchant has either completed this set of meal bundles, which are ready for pick up, or the meals are not ready. Therefore, drivers may wait W_{fp} amount of time or experience no waiting time at the merchant's location before they physically collect the meals. This amount of time W_{fp} is called the waiting time due to the delay in food preparation. Finally, drivers deliver the meals to customers sequentially and customers experience an average $W_{c,d}$ amount of delivery time. Similar to customers, drivers also experience a matching time $W_{v,q}$, a return-pickup time W_p, and a delivery time $W_{v,d}$. Drivers are not subject to waiting for accumulation because they are assigned delivery tasks after the order accumulation process, which means that the order accumulating process should have been completed before drivers were matched to any of the bundles.

To make the workflow clearer, we present two examples for customers and drivers, respectively.

Example 1 (Customer)**.** *One customer orders their food from a merchant at a time t_0. After this customer finishes payment, there will be a short waiting time to wait for accumulating a bundle until t_1. Then the accumulation time is $t_1 - t_0$. When a bundle is packed, it will be submitted into the platform's matching pool where there are multiple bundles and drivers. Then, the platform performs matching using some designated algorithm to match the most suitable driver to deliver this bundle. When a bundle is successfully matched with a driver at t_2, the matching process ends and the matching time is $t_2 - t_1$. In reality, OFD apps will normally show the order status as "pending" or "preparing" when the platform is performing accumulating or matching. After a driver is found, the order status will be changed to "driver heading for pick up" or other similar representations which vary across different platforms until the driver arrives at the restaurant at time t_3. If the meal is ready, the driver will collect the meal and start delivery and wait otherwise until t_4. In other words, if there is no waiting time for food preparation, $t_4 = t_3$, and if there is, $t_4 > t_3$. The food preparation time is thus $\max(t_4 - t_3, 0)$. Finally, the customer waits for the food until it is delivered on time t_5 and the customer delivery time is $t_5 - t_4$.*

Example 2 (Driver)**.** *One driver may start their status from "vacant" status on T_0 which means they are waiting to be matched. If the market presents a situation where there are more vacant drivers than needed (which is termed as "supply-dominated" situation, see Section 4.1.1 for details), drivers typically need to wait to be matched for a longer time than customers need to (because to maintain a certain service level, platforms usually keep the number of vacant drivers more than number of customer bundles). After being matched on time T_1 (matching time is $T_1 - T_0$), the driver is assigned a bundle of orders and heads to the restaurant for pickup. After the driver arrives at the restaurant on time T_2 (pickup time is $T_2 - T_1$), similarly, depending on whether the meal is ready or not, the driver collects the meal at T_3 which can be $T_3 > T_2$ if the meal is not ready or $T_3 = T_2$ if the meal is ready to go. The waiting time for food preparation is $\max(T_3 - T_2, 0)$. Then, the driver delivers all the orders and completes delivery at T_4, and the driver delivery time is $T_4 - T_3$. Since the driver needs to deliver all the orders in the bundle, the driver delivery time is greater than the customer delivery time.*

As shown in Figure 1, customers may experience $W_{c,a}$, which represents customers' order accumulation time, $W_{c,q}$ customers' matching time, W_p return-pickup time, W_{fp} food preparation time, and $W_{c,d}$ customers' delivery time. Food delivery drivers may experience $W_{v,q}$, which represents driver matching time, W_p return-pickup time, W_{fp} food preparation time, and $W_{v,d}$ the driver delivery time. Let W_c and W_v be the total waiting time experienced by customers and the total

time experienced by drivers, respectively. They can be expressed in Equation (1) and Equation (2) as follows:

$$W_c = W_{c,q} + W_{c,d} + W_p + W_{fp} + W_{c,a}, \tag{1}$$

$$W_v = W_{v,q} + W_{v,d} + W_p + W_{fp}. \tag{2}$$

3.2 Customer demand

Customer demand for each merchant i follows a demand density rate $\delta_i(r)$ in the unit of [order/(km^2· hour)], which is a function of the distance from the customer to the selected merchant r. We perceive restaurants as either a single restaurant or potentially being clusters of restaurants, similar to a food court or a shopping mall where restaurants are in close proximity such that the traveling time between restaurants is negligible. This viewpoint aligns more closely with reality and practically facilitates the process of order bundling. Nonetheless, to avoid confusion, we continue to refer to these entities simply as a "merchant" or "restaurant". In many North American cities, food courts or business areas often house multiple restaurants within the same urban plaza. Given that the meals are prepared and ready for delivery, the travel time between these restaurants is negligible. Similarly, in East Asia, shopping malls located in urban areas frequently feature numerous restaurants operating on the lower ground floor. This arrangement is particularly convenient for delivery drivers. Consequently, the density of such food courts or shopping malls should not be very high. Also, we consider independent customer demand for merchants under the assumption that the restaurant clusters are not very densely distributed. In other words, customers preferring one restaurant do not necessarily prefer another. This reflects a scenario where each merchant serves a distinct customer base, simplifying the model while allowing the analysis of individual merchant behavior. This assumption avoids complexities related to inter-merchant interactions, ensuring analytical tractability and enabling general insights into system performance. While this excludes interdependencies, such as geographic proximity or merchant competition, these could be addressed in future work with a more detailed model. By combining this assumption with a uniform customer distribution around each merchant, the model remains focused on key operational features while staying analytically manageable. The demand density rate can take various forms; for instance, decreasing with r, or first increasing and then decreasing with r. Using the demand density rate, the realized customer demand of all merchants is computed as the summation of all individual merchants:

$$q = \sum_{i=1}^{M} \int_0^R \delta_i(r) 2\pi r \, \mathrm{d}r. \tag{3}$$

In the model property part of this paper, for the sake of analytical tractability, we base our analysis on the assumption of homogeneous customer demand for each merchant, which is helpful in generating valuable insights using the model. In practice, this assumption can be relaxed and the value of $\delta_i(r)$ can be calibrated using real data.

3.3 Waiting times

3.3.1 Order accumulation time

The average customer's order accumulation time is computed as the time for the k^{th} order's arrival divided by 2 to consider the average between the luckiest (the customer enters the market as the

k^{th} order and does not need to wait) and the worst case (the customer enters the market as the 1st order and must wait to accumulate $k-1$ orders) for each customer when they order foods from merchants. Let $\overline{N}_w$ be the average number of working drivers during equilibrium and thus $q/\overline{N}_w$ is the average service rate for each working driver (equivalently for each bundle because each working driver should carry one bundle). Then, the customer's average accumulation time is

$$W_{c,a} = \frac{k-1}{2\left(q/\overline{N}_w\right)}. \tag{4}$$

3.3.2 Matching time

Customers' and driver expected matching times are expressed as follows:

$$W_{c,q} = \frac{1}{2}\tau p_c + \frac{3}{2}\tau p_c(1-p_c) + \frac{5}{2}\tau p_c(1-p_c)^2 + \cdots = \tau\left(\frac{1}{p_c} - \frac{1}{2}\right), \tag{5}$$

$$W_{v,q} = \frac{1}{2}\tau p_v + \frac{3}{2}\tau p_v(1-p_v) + \frac{5}{2}\tau p_v(1-p_v)^2 + \cdots = \tau\left(\frac{1}{p_v} - \frac{1}{2}\right), \tag{6}$$

where p_c or p_v are the probabilities of each bundle of customers or each driver being successfully matched within each match time interval, respectively, and we assume that the customers and drivers follow a uniform arrival rate and this rate is large enough relative to the matching time interval, which makes it possible to approximate the arrival processes as a (deterministic) fluid model (Shortie et al., 2018, pp 392). Equations (5) and (6) show that the matching time is the expected value (sum of probability multiplied by outcome) of being matched on each matching interval.

The matching probabilities are distinct in two scenarios, the supply-dominant (SD) scenario and the demand-dominant (DD) scenario. The division of the two scenarios is based on the relative relationship between the number of vacant drivers N_v and the number of order bundles N_b at the end of each matching interval. We will provide a formal definition and differentiation criteria in Section 4. In a supply-dominant scenario, N_v exceeds N_b and thus all order bundles are guaranteed a match with certain drivers. Consequently, the probability of a customer match, denoted as p_c, is 1 (i.e., $p_c = 1$). Under this circumstance, driver matching probability, denoted as p_v, equals N_b/N_v. This is calculated by the principle of conservation between matched drivers and order bundles $p_v N_v = p_c N_b$. In contrast, in the demand-dominated scenario, we have $N_v < N_b$. Then, all the vacant drivers are matched and $p_v = 1$, resulting in the customer's matching probability $p_c = N_v/N_b$. With these two scenarios defined, we know that the number of matched drivers for each matching interval (and equivalently, the number of matched order bundles) is $\min(N_b, N_v)$.

3.3.3 Delivery and return-pickup time

Delivery behavior under order bundling is an essential part of the modeling process. Insights from the literature argue that the delivery process in the OFD market is highly dependent on the driver's local knowledge and experience (Mao et al., 2019; Liu et al., 2021; Mao et al., 2022; Carlsson et al. (2024)). As a result, we assume that drivers serve for a specific region and exclude the driver repositioning process. This assumption can be justified by the practice in the real world, where OFD platforms often restrict the service region for drivers to ensure efficient and reliable services (e.g., Uber Eats' "delivery zone" (Uber Technologies Inc., 2025)).

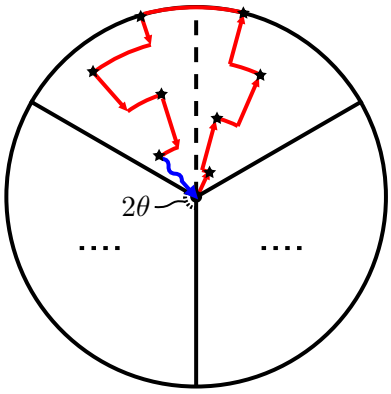

Figure 2: Delivery and return-pickup routing approximations. Red lines represent the approximated delivery route and wavy blue lines represent the approximated return-pickup route. Black stars represent customers' locations, and the black dot in the center is the location of the merchant.

We adopt continuum approximation to calculate the delivery and return-pickup length, similar to the approaches by Wang and Odoni (2016), Chen and Wang (2018), Bahrami et al. (2023), and Ke et al. (2024). Delivery and pickup routes are assumed to be in one trip, and route lengths are denoted as L_d and L_p for delivery and return-pickup routes respectively. Figure 2 depicts the approximations of delivery and return-pickup schemes. The routing indicates that drivers deliver the first half of customers. Afterward, they return to the merchant while simultaneously delivering the remaining half of the customers. Simulation experiments also validate the return behavior in Figure 2 that under a general VRP without returning (also called open-VRP) problem, the last drop-off destination will be closer than the farthest delivery destination (Appendix C). The simulation experiment indicates that on average, drivers will follow a return-like route, and enhance the applicability of our approximation in Figure 2. Also, if we consider a uniform distribution of restaurants across the space, we can assume that drivers would stay at their last delivery destination after the completion of a bundle delivery. On the one hand, since the restaurants are uniformly distributed, drivers do not have the preference of which restaurant to go to, and they would decide to stay at the last drop-off location. On the other hand, this approach is a modeling tool to ensure fair comparison between different strategies and maintain analytical tractability. Under the assumption that restaurant distribution is sparse (Section 3.2), we can just consider the matching result that drivers will ultimately be matched to the original restaurant. The continuum approximation technique allows us to deal with uncertain delivery points and calculate the average delivery distance with continuous R and k. This adopted approximation scheme might not be the most accurate but it reflects the most important impact of both the maximum delivery distance and the bundling ratio, i.e., the relative position and number of detours needed to be made.

The delivery area of a merchant is assumed to be a circular disk and can be divided into several sectors (Bahrami et al., 2023), each of which is the individual delivery area of one driver. This is interpreted as the platform assigning a suitable area (which can be narrow or wide) to each driver—and thus an optimized visiting sequence of orders—to improve delivery efficiency. In practice, even though it is possible that there are overlapping delivery areas among different drivers, the platform can partition the region and optimize the routing of each driver (e.g., Carlsson et al. (2024)) to avoid overlapping (if two routes are overlapped, orders in one route can be simply switched to another driver which reduces detour). We also assume that the driver fleet size is greater than the number of merchants, $N > M$, to ensure that there will always be at least one driver on average serving each merchant. If customer demand is high, each driver will be in charge of a narrow sector

because the number of customers in this narrow sector can reach the bundling ratio k. In contrast, for low demand, each driver's individual delivery area will be wide (the inner angle is large) because customers are distributed sparsely. The inner angle of each of the sectors is denoted as 2θ, and 2θ is given by 2π divided by the average number of working drivers per merchant under equilibrium. The inner angle thus needs to satisfy the condition that $\theta < \pi$, meaning that each food delivery driver serves a delivery area of at most one merchant. An inner angle θ greater than π represents that the food delivery supply from each individual driver has exceeded the food delivery demand of a single merchant, indicating that the food delivery demand is too small. This scenario is regarded as invalid in this study. Let the average total number of working drivers in each matching interval be denoted as $\overline{N}_w$; this inner angle is computed by

$$2\theta = \frac{2\pi}{\overline{N}_w/M} = \frac{2\pi M}{\overline{N}_w}, \tag{7}$$

where the average number of working drivers $\overline{N}_w$ is divided by M to represent the average number of working drivers serving each merchant.

Delivery distance consists of a transverse part (L_t) and an axial part (L_a). Using the continuum approximation (CA) method, following Newell and Daganzo (1986), Jabali et al. (2012), and Bahrami et al. (2023), the average transverse (tangential) travel distance of a driver who is r away from the merchant is $l_r = r\theta/3$. The probability p_r of each customer's appearing between radius r and $r + \mathrm{d}r$ for each merchant is $p_r = 2\pi r\,\mathrm{d}r\delta_i(r)/q_i$, where q_i is the realized customer demand rate of merchant i. Then the expected transverse distance of each driver is

$$l_t = \int_{r=0}^{r=R} p_r l_r = \int_0^R \frac{2\pi r^2 \theta \delta_i(r)}{3q_i}\,\mathrm{d}r. \tag{8}$$

The driver will transversely travel on average k times because they will visit k customers on average (we consider CA and treat k as a continuous variable for approximation purpose), and thus the total transverse distance is

$$L_t = kl_t. \tag{9}$$

Meanwhile, each driver also needs to travel an axial distance from the center to the outskirts of the delivery area (excluding the return-pickup distance):

$$L_a = 2R - L_p, \tag{10}$$

where L_p denotes the return-pickup distance. We formulate the return-pickup distance as a fraction of the maximum delivery distance divided by the number of orders in each half-sector, or interpret it as a fraction of the average axial spacing between each customer on one side of the sector (shown as the blue line with an arrow in Figure 2):

$$L_p = \eta\frac{R}{k/2} = \frac{2R\eta}{k}, \tag{11}$$

where η is a coefficient, which is dependent on the demand profile and can be estimated using real-world data and also used to calibrate the return-pickup length of drivers. Considering η is just an exogenous coefficient, we take the value $\eta = 1$ in the modeling solution to maintain a neat and interpretable form of analytical results.

Finally, driver delivery time and return-pickup time are the delivery distance and return-pickup distance divided by the average speed (assumed to be a constant, v), which gives[1]

$$W_{v,d} = \frac{L_d}{v} = \frac{L_t + L_a}{v} = \frac{1}{v}\left(2R + k\int_0^R \frac{2\pi r^2 \theta \delta_i(r)}{3q_i}\,\mathrm{d}r - L_p\right), \tag{12}$$

$$W_p = \frac{L_p}{v} = \frac{2R\eta}{kv}. \tag{13}$$

For each customer, the average delivery time is the sum of the delivery time for all customers divided by k. The delivery distance for the n^{th} customer depends on which half of the sector the customer is in. Readers are referred to the left-hand side of Figure 2 for an illustration. The formulation is

$$W_{c,d,n} = \begin{cases} nL_p + (n-1)l_t, & n \le \dfrac{k}{2}, \\ (n-1)L_p + nl_t, & n > \dfrac{k}{2}. \end{cases} \tag{14}$$

Then, the average customer delivery time is computed as (see proof in Appendix A)

$$W_{c,d} = \frac{L_p + L_d + 2R(\eta - 1)}{2v}. \tag{15}$$

3.3.4 Waiting time due to food preparation

Within the merchant's operations, there is a capacity limit for the food preparation rate, which leads to a potential scenario in which drivers may arrive at the merchant but have to wait until all meals in a bundle are ready. This waiting time, denoted W_{fp}, should adhere to the condition that the order arrival rate amortized on each merchant, q/M, does not exceed the food preparation rate, $1/\tau_M$ (i.e., $q/M \le 1/\tau_M$) where τ_M denotes the average time to complete one order of food. This constraint is essential to avoid an over-saturated demand that prevents the system from reaching a steady state.

To ensure efficient order processing, each merchant initiates meal preparation immediately upon receiving an order . Once the last customer in a bundle places an order, successfully completing the bundle, the platform will promptly call for drivers to pick up the bundle (i.e., initiating matching). Simultaneously, the restaurant will start cooking the last meal.

On the platform's side, there are matching times experienced by customers $W_{c,q}$ and the return-pickup time W_p, which contiguously happen after the order request of the last customer in a bundle. Therefore, it takes $W_{c,q} + W_p$ in total from the start time of the call for matching to the time the assigned driver arrives at the restaurant. On the restaurant's side, the meal is being prepared with an average time τ_M for the merchant to finish. We can approximate the order arrival-preparation process as a fluid model (Shortie et al., 2018, pp 392) for the derivation of analytical insights. Therefore, W_{fp} is calculated from the difference between τ_M and $W_{c,q} + W_p$. Also, it should be non-negative, which gives rise to

$$W_{fp} = \max\left(\tau_M - W_{c,q} - W_p, 0\right). \tag{16}$$

[1] We acknowledge that the following equations are based on approximation techniques, which might generate some bias. Our use of these approximations is for illustrative purposes with closed-form solutions and valuable analytic insights.

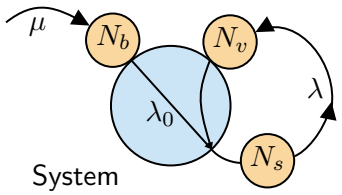

Figure 3: Illustration of the system under equilibrium. N_v and N_s are the numbers of drivers who are awaiting matching and meal preparation respectively.

3.4 Equilibrium conditions

In the steady state of the system (equilibrium), all customer demand is satisfied with market clearing (Yang et al., 2010, Yang and Yang, 2011) achieved based on the following conditions. First, regarding the matching equilibrium, realized bundle-wise customer demand rate q/k should be equal to the matching rate λ_0 (it is also the rate at which drivers transfer from the vacant status to the working status). Second, regarding the self-consistency of the transfer rate between working drivers and vacant drivers, the matching rate λ_0 should be equal to the rate at which working drivers transfer to vacant drivers λ:

$$q/k = \lambda_0, \tag{17}$$

$$\lambda_0 = \lambda. \tag{18}$$

Through these two equations, we obtain the equality condition that $q/k = \lambda$. Since customers order food online and induce traffic, we treat it as demand for the movement of meals, termed *food delivery demand (rate)*. In contrast, the pickup-delivery process, which transports meals from merchants to customers, can be considered to be supply for the movement of meals; thus we call it *food delivery supply (rate)*. Note that food delivery demand (or supply) here is not the same concept used to define the DD (or SD) scenario, in which the former is a rate while the latter is a quantity (mass). Then, the equality condition $q/k = \lambda$ is interpreted as the food delivery supply meeting the food delivery demand.

Figure 3 illustrates the equilibrium process of the OFD market, in which on the left customer demand flows into the system at a rate of q, and on the right delivery drivers are moving meals out of the system to customers at a rate of λ. Within the system, shaded in blue, customer demand rate q/k and vacant driver arrival rate λ are both equal to the matching rate λ_0.

According to our discussion in Section 3.3.2, the number of matched vacant drivers (or equivalently, the number of matched bundles) is equal to $\min(N_b, N_v)$. Since the matching time interval is τ, the matching rate is $\lambda_0 = \min(N_b, N_v)/\tau$. Vacant drivers are subject to $W_{v,q}$—the waiting time to be matched—where $W_{v,q} = \tau(1/p_v - 1/2)$ (see Section 3.3.2). Since $p_v N_v = p_c N_b$, we have $W_{v,q} = \tau(N_v/N_b - 1/2)$ if $N_v \geq N_b$ and $W_{v,q} = \tau/2$ if $N_v < N_b$. For $N_v \geq N_b$, we have

$$W_{v,q} = \tau\left(\frac{N_v}{N_b} - \frac{1}{2}\right) = \frac{N_v}{N_b/\tau} - \frac{\tau}{2} = \frac{N_v}{\lambda_0} - \frac{\tau}{2}. \tag{19}$$

Rearranging Equation (19), we obtain

$$N_v = \lambda_0\left(W_{v,q} + \frac{\tau}{2}\right). \tag{20}$$

Similarly, $N_b = \lambda_0 (W_{c,q} + \tau/2)$ can also be derived from Equation (5). Apart from the matching equilibrium, we have another condition: vehicle conservation. We hold the assumption of a constant vehicle fleet size because our primary emphasis is the influence of the service region and the bundling ratio; examination of the behavior of the fleet size is reserved for future work. Then we have

$$N = \lambda W_v = \lambda (W_{v,q} + W_p + W_{fp} + W_{v,d}). \tag{21}$$

Combining Equations (18), (20) and (21), we obtain the following condition regarding the rate of the working drivers:

$$N - N_v = \lambda \left(W_p + W_{fp} + W_{v,d} - \frac{\tau}{2} \right). \tag{22}$$

Finally, with food delivery demand-supply equality $q/k = \lambda$, Equation (20), and Equation (22), we define the equilibrium of the OFD market below.

Definition 1. *For an OFD market, the matching between order bundles and vacant drivers, as well as the food delivery demand-supply, are considered to achieve a stationary equilibrium state and there is market clearing if the following conditions hold.*

$$\frac{q}{k} = \frac{N_v}{W_{v,q} + \frac{\tau}{2}} \text{ (demand-matching equilibrium)}, \tag{23a}$$

$$\frac{q}{k} = \frac{N - N_v}{W_p + W_{v,d} + W_{fp} - \frac{\tau}{2}} \text{ (demand-supply equilibrium)}. \tag{23b}$$

It should be satisfied that the number of vacant drivers and the number of order bundles should be greater than the number of matched drivers/bundles in each matching interval, $\lambda\tau$—i.e., $N_b \geq \lambda\tau, N_v \geq \lambda\tau$. This equilibrium model has two degrees of freedom, N_v and N_b; once they are fixed, the system, as well as its endogenous variables, are all determined. Therefore, we treat N_v and N_b as two unknown variables and solve them using the equilibrium conditions.

4 Model solution and properties

We treat N_v and N_b as two unknown variables, as described in the previous section. The model solution is defined as follows.

Definition 2. *The model solution is the set of N_v and N_b such that the equilibrium conditions in Equation (23) are satisfied under a given set of decision variables, i.e., R and k.*

Since we adopt CA to approximate the delivery and pickup distances, their detailed expressions are dependent on the customer demand profile $\delta(r)$; model solutions also are. $\delta(r)$ can take various forms in different geographic locations and at different times. For the sake of deriving analytical insights, we specify this demand profile to be uniform across the space, which is defined as follows:

$$\delta(r) = \begin{cases} \dfrac{\overline{q}}{M\pi R_a^2}, & r \leq R_a, \\ 0, & r > R_a, \end{cases} \tag{24}$$

where $\overline{q}$ denotes the potential customer demand over the entire region, M denotes the number of merchants, and R_a is the radius of the merchant's attractive region beyond which there is no demand. We assume in a tactical operation, which has impact on market performance but not yet on long-term effects such as customer complaints and demand decrease. We also assume that customer demand is homogeneous for analytical tractability and thereby all merchants share the same demand density rate δ; this assumption can be relaxed if real data on customer demand is known. We consider $\eta = 1$ in the model solution and properties for illustrative purposes for a neat representation of analytical results, which also facilitates the development of analysis. Despite adopting these assumptions in the model's solutions and properties, we demonstrate numerical results in the appendix (see discussion in Appendix B), where we consider different demand density rates and the stochasticity of customer's arrival to food preparation rate, respectively.

4.1 Existence of the solutions and four scenarios for the OFD market

The existence of the equilibrium solution depends on whether the system can reach an equilibrium state—i.e., whether the food delivery supply can meet the food delivery demand. We define the system with an equilibrium solution as a stable system. In a stable system, since the food delivery supply is sufficient, all realized customer demand q can be served. In contrast, not all of q can be satisfied in an unstable system, which is not desired and it may produce a large amount of waiting time for customers.

Insights of R and k into the existence of the equilibrium solution. Given the maximum delivery distance R, a small bundling ratio k may risk the OFD system's being unstable due to insufficient delivery supply. On the other hand, given k, a large R may risk the OFD system's being unstable due to excessive customer demand.

R represents the maximum delivery distance and can eliminate some customer demand outside the delivery area of a merchant. Therefore, a large R will cover a large customer demand and thus a large demand for transporting meals from the merchant to customers. The bundling ratio k reveals how many orders each driver carries on each delivery, and hence contributes positively to the delivery supply. If k is not sufficiently large, a system may be subject to the risk that the food delivery supply cannot meet the food delivery demand. Consequently, there is a bundling ratio threshold k_c for any given R in order to achieve system stability. The existence condition of the system equilibrium is defined as follows (see the expression of k_c in Appendix D).

Lemma 1 (**Existence condition**). *Given R, the equilibrium solution of the system exists if $k \geq k_c$, where k_c is a function of R—i.e., $k_c = k_c(R)$—and we have* $\dfrac{\partial k_c}{\partial R} > 0$.

Proof. See Appendix D. □

We focus on the effects from R and k which reflect the size of the service region and the number of orders each driver carries because according to our results in Tables 2 to 4. In other words, we analyze the system and discuss the properties in the two-dimensional coordinate space of R and k:

$$\mathcal{S} = \{(R,k) | R \geq 0, k \geq 2\}. \tag{25}$$

Let $\mathcal{L}_e \subset \mathcal{S}$ represent the relationship between R and k of k_c, $\mathcal{L}_e$ serves as the boundary curve in $\mathcal{S}$ for the system to be stable. We have $\mathcal{L}_e = \{(R,k) | N_v = \lambda\tau \text{ and } W_{fp} = 0\}$ where the subscript e stands for *equilibrium*.

4.1.1 Four scenarios for the OFD market

We differentiate the OFD market into four distinct scenarios, based on two criteria. The first concerns the food delivery supply–demand relationship, which is based on whether $N_b > N_v$ (demand-dominant, DD) or otherwise (supply-dominant, SD). The second criterion concerns whether food delivery drivers have to wait at the restaurant for meal preparation when they arrive at the restaurant, depending on whether $W_{fp} = 0$ (ready-for-pickup, RP) or not (wait-for-pickup, WP).

Let $\mathcal{L}_{RP,WP} \subset \mathcal{S}$ be the boundary curve that separates the decision space of the RP scenario and the WP scenario, and $\mathcal{L}_{SD,DD} \subset \mathcal{S}$ be the boundary curve that separates the decision space of the SD scenario and the DD scenario, we obtain the following property.

Lemma 2. *The model solution is continuous at any point on $\mathcal{L}_{RP,WP}$ and on $\mathcal{L}_{SD,DD}$.*

Proof. See Appendix E. □

The criterion of whether N_b is greater than N_v. Since the SD scenario and the DD scenario are differentiated by the relative value of N_b and N_v, as discussed in Section 3.3.2, the critical condition for the SD scenario and the DD scenario is $N_b = N_v$. Substituting $N_b = N_v$ in Equation (23), we obtain

$$N_b = N_v = \lambda\tau, \tag{26}$$

$$\frac{N}{\lambda} - \frac{\tau}{2} = (W_p + W_{v,d} + W_{fp})|_{N_b = N_v = \lambda\tau}. \tag{27}$$

Simplifying Equation (27) yields $\Delta_c(R,k) = 0$, where $\Delta_c(R,k)$ is a function of decision variables R and k, and it only depends on exogenous variables (see its formulation in Appendix F). We then introduce the criterion for differentiating SD and DD scenarios—the demand-supply mass relationship (DSMR) criterion based on $\Delta_c(R,k)$, as follows (see the expression of Δ_c in Appendix F).

Lemma 3 (DSMR criterion). *For a stable system satisfying Lemma 1, the system is considered to be under the SD scenario if the condition $\Delta_c(R,k) \le 0$ is satisfied; otherwise, it is considered to be under the DD scenario. $\mathcal{L}_{SD,DD}$ corresponds to $\Delta_c(R,k) = 0$.*

Proof. See Appendix F. □

Also, the boundary curve $\mathcal{L}_{SD,DD} \subset \mathcal{S}$ has the following property.

Lemma 4. *In the R-k coordinate system of $\mathcal{S}$, the boundary curve $\mathcal{L}_{SD,DD}$ has a slope greater than 0, i.e., $\dfrac{\mathrm{d}R}{\mathrm{d}k} > 0$.*

Proof. See Appendix G. □

The criterion of whether drivers need to wait for food preparation. The RP scenario and the WP scenario are differentiated based on whether $W_{fp} = 0$, i.e., whether $\tau_M - W_p - W_{c,q} \le 0$. Then, given that k_c (see its expression in Appendix Section D) is the critical k to make the equilibrium exist, we have the following RPWP criterion.

Lemma 5 (**RPWP criterion**). *For an OFD system under the SD scenario given by Lemma 3, if the condition* $\tau_M - \frac{2R\eta}{kv} - \frac{\tau}{2} \leq 0$ *is satisfied, the system is under the RP scenario. Otherwise, the system is under the WP scenario. For an OFD system under the DD scenario given by Lemma 3, the system is under the RP scenario if* $k = k_c(R)$ *and under the WP scenario if* $k > k_c(R)$.

Proof. See Appendix H. □

With the DSMR criterion defined in Lemma 3 and the RPWP criterion defined in Lemma 5, the OFD system is now categorized into four scenarios: the RP-SD scenario, WP-SD scenario, RP-DD scenario, and WP-DD scenario. Remarkably, since the existence condition requires that $N_v + \lambda W_{fp} \geq \lambda\tau$, which results in the critical condition's being $N_v = \lambda\tau$ and $W_{fp} = 0$, the condition $N_v = \lambda\tau$ for the system under the RP scenario is equivalent to the condition $\tau_M - W_P - W_{c,q}$ for the system under the DD scenario. We provide equilibrium solutions and analyses of these scenarios in the next section.

4.2 Equilibrium solutions

This section provides the closed-form solution for the two intermediate unknown variables, N_b and N_v, using the equilibrium conditions in Equation (23):

$$\frac{q}{k} = \frac{N_v}{W_{v,q} + \frac{\tau}{2}},$$
$$\frac{q}{k} = \frac{N - N_v}{W_p + W_{v,d} + W_{fp} - \frac{\tau}{2}}.$$

The problem has distinct formulations for each scenario—the RP-SD scenario, WP-SD scenario, RP-DD scenario, and WP-DD scenario.

The RP-SD scenario. If the system is subject to decision variables that cause the system to be under the RP-SD scenario according to the criteria in Lemma 3 and Lemma 5, we have $N_v \geq N_b$ and $\tau_M - \frac{2R\eta}{kv} - \frac{\tau}{2} \leq 0$. Then the equilibrium solutions for N_v and N_b are

$$N_v = \overbrace{N}^{\text{Fleet size}} - \overbrace{\frac{6Rq - 3q\tau v + 2\sqrt{2\pi MRk^2qv + 9R^2q^2}}{6kv}}^{\substack{\text{Average \# of return-pickup} \\ \text{and delivery drivers}}}, \tag{28}$$

$$N_b = \frac{q}{k}\tau. \tag{29}$$

Equation (28) also tells that the average number of working drivers $\overline{N}_w = N - N_v + \lambda_0\tau/2 = \frac{Rq}{kv} + \sqrt{\frac{2\pi MRq}{9v} + \left(\frac{Rq}{kv}\right)^2}$, influenced by the number of drivers on their delivery and return-pickup routes.

The WP-SD scenario. If the system is subject to decision variables that cause the system to be under the WP-SD scenario according to the criteria in Lemma 3 and Lemma 5, we have $N_v \geq N_b$ and $\tau_M - \frac{2R\eta}{kv} - \frac{\tau}{2} > 0$. Then the equilibrium solutions for N_v and N_b are

$$N_v = \overbrace{N}^{\text{Fleet size}} - \frac{\overbrace{6R_sq - 3q\tau v + 2\sqrt{2\pi MRk^2qv + 9R_s^2q^2}}^{\substack{\text{Average \# of return-pickup, delivery,} \\ \text{and awaiting (for meal preparation) drivers}}}}{6kv}, \tag{30}$$

$$N_b = \frac{q}{k}\tau, \tag{31}$$

where $R_s = R + W_{fp}v/2$. Similar to the RP-SD scenario, from Equation (30) we know the average number of working drivers $\overline{N}_w = \frac{R_sq}{kv} + \sqrt{\frac{2\pi MRq}{9v} + \left(\frac{R_sq}{kv}\right)^2}$, influenced by the number of drivers on their delivery and return-pickup routes.

The RP-DD scenario. If the system is subject to decision variables that cause the system to be under the RP-SD scenario according to the criteria in Lemma 3 and Lemma 5, we have $N_v < N_b$ and $k = k_c(R)$. Then the equilibrium solutions for N_v and N_b are

$$N_v = \overbrace{N}^{\text{Fleet size}} - \frac{\overbrace{6Rq - 3q\tau v + 2\sqrt{2\pi MRk^2qv + 9R^2q^2}}^{\substack{\text{Average \# of return-pickup} \\ \text{and delivery drivers}}}}{6kv} = \frac{q}{k}\tau, \tag{32}$$

$$\underbrace{N_b}_{\substack{\text{Part of the \# of} \\ \text{drivers awaiting} \\ \text{food preparation}}} = \underbrace{\frac{q}{k}\left(\tau_M - \frac{2R\eta}{kv} + \frac{\tau}{2}\right)}_{\substack{\text{Remainder terms of the \# of} \\ \text{drivers awaiting food preparation}}}, \tag{33}$$

where Equation (33) means that the food preparation time should be exactly equal to the pickup time and customers' matching time. This equation renders the RP-DD scenario a special case of the WP-DD scenario (the waiting time for food preparation is 0).

The WP-DD scenario. If the system is subject to decision variables that cause the system to be under the WP-DD scenario according to the criteria in Lemma 3 and Lemma 5, we have $N_v < N_b$ and $k > k_c(R)$. Then the equilibrium solutions for N_v and N_b are

$$N_v = \frac{q}{k}\tau, \tag{34}$$

$$\begin{aligned} \underbrace{N_b}_{\substack{\text{Part of the \# of} \\ \text{drivers awaiting} \\ \text{food preparation}}} = & \underbrace{\frac{4\pi MRkq}{18Nkv - 9q\tau v} + \frac{2R}{v}\cdot\frac{q}{k}}_{\substack{\text{\# of return-pickup} \\ \text{and delivery drivers}}} - \underbrace{\left(N - \frac{q\tau}{2k}\right)}_{\substack{\text{Average \# of} \\ \text{working drivers}}} \\ & + \underbrace{\frac{q}{k}\left(\tau_M - \frac{2R\eta}{kv} + \frac{\tau}{2}\right)}_{\substack{\text{Remainder terms of the \# of} \\ \text{drivers awaiting food preparation}}}. \end{aligned} \tag{35}$$

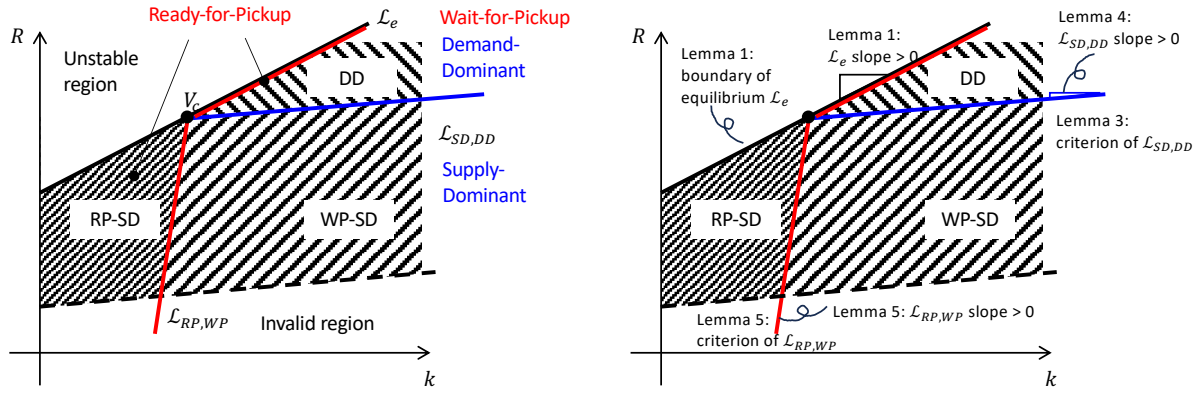

(a) Division names **(b)** Illustration of lemmas

Figure 4: Diagram for the division of the different scenarios. The "invalid region" (refer to Section 3.3.3) corresponds to $\theta > \pi$ and falls outside the scope of this study.

Equation (32) of the RP-DD is on the boundary curve $\mathcal{L}_e$, as previously in Lemma 5 (we can also validate the solution of N_b by substituting $k = k_c$ in Equation (35) and then obtain Equation (33)). It is also intuitively true that if there are drivers awaiting, demand should not be dominated because there is still unused delivery supply in the system. For brevity, we combine the RP-DD scenario and the WP-DD scenario to be the DD scenario and analyze them as a whole.

4.3 Uniqueness of the solution

We next discuss the uniqueness of the equilibrium solutions. We know from Lemma 3 and Lemma 5 that the separation curves $\mathcal{L}_{RP,WP}$ and $\mathcal{L}_{SD,DD}$ are exclusively dependent on the decision variables under certain exogenous variables, which indicates that there is no overlapped region between the RP and WP scenarios, or between the SD and DD scenarios. We then have the following proposition.

Proposition 1. *Given a set of certain decision variables (R,k), the equilibrium solution of the OFD system is unique if the existence condition in Lemma 1 is met and the regions of the RP-SD scenario, WP-SD scenario, and DD scenario are mutually exclusive in $\mathcal{S}$.*

Proof. See Appendix I. □

Each of the three scenarios (RP-SD, WP-SD, DD) in $\mathcal{S}$ is located in R-k coordinate system as shown in Figure 4. A large R entails more customer demand for the restaurant, and thus the demand-dominant scenario is more likely to happen. This leads to the region of the WP-DD scenario located above the region of the WP-SD scenario in the R-k coordinate system. A large k reflects that there will be more customer orders to be delivered, with less average spacing between each customer. This potentially reduces the average return-pickup distance, which causes $W_{fp} = \tau_M - W_p - W_{c,q}$ to tend to be larger. Therefore, an increase in k may bring the scenario from the RP-SD scenario to the WP-SD scenario. These three scenarios spread in the R-k coordinate system, as shown in Figure 4 and the above discussion. The intersection point V_c is also on the

Table 2: Properties of the system under the RP-SD scenario

Variables	N_v	N_b	W_p	$W_{c,a}$	$W_{c,q}$	$W_{v,q}$	$W_{c,d}$	$W_{v,d}$	W_c	W_v	λ
R	$\downarrow$	$\uparrow$	$\uparrow$	$\searrow\nearrow$	$\rightarrow$	$\downarrow$	$\searrow\nearrow$	$\searrow\nearrow$	$\searrow\nearrow$	$\downarrow$	$\uparrow$
k	$\uparrow$	$\downarrow$	$\downarrow$	$\uparrow$	$\rightarrow$	$\uparrow$	$\uparrow$	$\uparrow$	$\uparrow/\searrow\nearrow$	$\uparrow$	$\downarrow$

Table 3: Properties under the WP-SD scenario (red arrows are those that differ from Table 2)

Variables	N_v	N_b	W_p	$W_{c,a}$	$W_{c,q}$	$W_{v,q}$	$W_{c,d}$	$W_{v,d}$	W_{fp}	W_c	W_v	λ
R	$\downarrow$	$\uparrow$	$\uparrow$	$\searrow\nearrow$	$\rightarrow$	$\downarrow$	$\searrow\nearrow$	$\searrow\nearrow$	$\downarrow$	$\searrow\nearrow$	$\downarrow$	$\uparrow$
k	$\uparrow$	$\downarrow$	$\downarrow$	$\uparrow$	$\rightarrow$	$\uparrow$	$\uparrow$	$\uparrow$	$\uparrow$	$\uparrow$	$\uparrow$	$\downarrow$

Table 4: Properties under the DD scenario (red arrows are those that differ from Table 3)

Variables	N_v	N_b	W_p	$W_{c,a}$	$W_{c,q}$	$W_{v,q}$	$W_{c,d}$	$W_{v,d}$	W_{fp}	W_c	W_v	λ
R	$\uparrow$	$\uparrow$	$\uparrow$	$\downarrow$	$\uparrow$	$\rightarrow$	$\uparrow$	$\uparrow$	$\downarrow$	$\downarrow$	$\downarrow$	$\uparrow$
k	$\downarrow$	$\downarrow$	$\downarrow$	$\uparrow$	$\downarrow$	$\rightarrow$	$\uparrow$	$\uparrow$	$\uparrow$	$\uparrow$	$\uparrow$	$\downarrow$

curve $\mathcal{L}_e$ because on V_c, $N_v = \lambda\tau$ and $W_s = 0$, which satisfies the existence condition represented by the curve $\mathcal{L}_e$.

4.4 Model properties

Properties of the decision variables are summarized in Table 2 through Table 4. In the tables, $\rightarrow$ denotes that the decision variables do not have an impact; $\uparrow$ or $\nearrow$ that the dependent variables increase with respect to the decision variables; and $\downarrow$ or $\searrow$ that the dependent variables decrease with respect to the decision variables. Also, we make a mild assumption that $R > \tau v$, because the matching interval is normally very small and drivers are not expected to travel to the border of the delivery area within a single matching interval.

Proposition 2. *In the SD scenario, some important properties of the OFD system are as follows:*

1. *Customer accumulation time first decreases and then increases with the maximum delivery distance R.*
2. *Customer delivery time first decreases and then increases with the maximum delivery distance R.*
3. *Customer total waiting time first decreases and then increases with the maximum delivery distance R.*
4. *In the RP-SD scenario, customer total waiting time monotonically increases with k when R is small, and first decreases and then increases with k when R is large.*

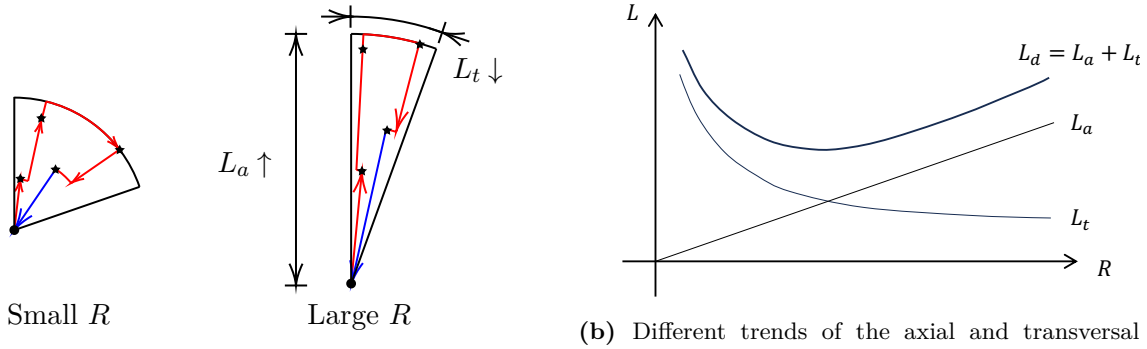

(a) Illustration of the impact of an increase in R

(b) Different trends of the axial and transversal travel distances

Figure 5: Depiction of insights into the maximum delivery distance.

Proof. See Appendices J–L. □

Insight of R into accumulation time. From the expression of customer accumulation time $W_{c,a} = \frac{k-1}{2(q/\overline{N}_w)}$, the non-monotonic relationship can be attributed to the different rate of change of q and $\overline{N}_w$ with respect to R because both of them increase with R. When R is relatively small, q increases slower than $\overline{N}_w$ does, and when R gets larger, the quadratic term of q makes it increase faster and surpass the rate of change of $\overline{N}_w$. Intuitively, the accumulation time is dependent on the customer demand of a sector of the circular delivery area. When R is small, it is conceivable that the sector is "fat", having a larger angle compared with that when R is large where the sector is "thin" (see Figure 5a as an illustration). If customer demand arrives at the space uniformly, the probability of a customer appearing at one specific sector is non-monotonically related to R. As R increases, although the total demand of a service region increases, the demand for each sector does not necessarily increase because the sector becomes thinner, which contributes to the non-monotonicity.

Insight of R into delivery time. Proposition 2.1 presents a non-monotonic relationship of delivery time with R. This is because of the change in each driver's individual delivery area. When the delivery radius R increases and the delivery area covers more customer demand, the number of working drivers N_w gets larger to fulfill the increased customer demand. When more drivers are involved in delivery, the platform can design better delivery routes (e.g., each driver only serves a narrow sector in the circular delivery region) to avoid some unnecessary detours—and thus shorter delivery time, as shown in Figure 5a. On the other hand, however, the increase in the delivery radius per se causes the delivery distance to be larger. These two trends in response to the change in R finally cause the delivery distance to behave non-monotonically from small to large R. In scenarios in which R is relatively small, the driver delivery area is not large enough, which results in each driver being allocated a relatively broad sector (as evidenced by the large inner angle θ). Under such circumstances, an increase in the delivery area may have a great impact on the transversal delivery distance associated with each driver. In contrast, in the context of large R,

the system features many working drivers with each in charge of a very narrow region. Therefore, any optimization efforts that target the transverse detour may not have significant influences as the increase in R itself. In this scenario, the line-haul distance emerges as the primary determinant that influences the delivery distance. As shown in Figure 5b, when R gets larger, the impact of the increase in transversal distance L_t tends to be small, and the delivery distance $L_d = L_a + L_t$ increases with R. The transition of the dominant influential factor causes the delivery time to be non-monotonic with R.

Insight of R into customer total waiting time. Customer total waiting time exhibits a non-monotonic relationship with R. Specifically, for smaller values of R (which represent a smaller service region and thus smaller demand), an increase in R correlates with a decrease in customer total waiting time. Conversely, for larger values of R (larger service region, larger demand), an increase in R results in an increase in customer total waiting time. This non-monotonic relationship can be attributed to the fact that W_c is the superposition of two major waiting times $W_{c,a}$ and $W_{c,d}$, and other minor waiting times (in SD scenario) such as W_p, $W_{c,q}$, and W_{fp}. Both of $W_{c,a}$ and $W_{c,d}$ have a non-monotonic relationship with R.

Insight into the bundling ratio. For a stable system, in which all the customer demand can be served, whether to bundle depends on customer demand. If customer demand is small, there is no need to bundle because the nature of bundling is to deal with large demand. This is shown in Figure 6a, where the optimal point corresponds to a bundling ratio less than 2, indicating that bundling is unnecessary. However, the bundling ratio does not always follow the rule "the larger the better." When the realized customer demand is high (i.e., R is large) while still maintaining the system stability, system operators may consider order bundling and there is a trade-off between (1) order accumulation and delivery time and (2) return-pickup time. Bundling requires an accumulation of orders and increases the delivery time. On the other hand, it reduces average return-pickup time because more customers in a bundle means shorter expected return-pickup distance from the last delivery's endpoint to the restaurant. When k is small, the effect of the return-pickup time dominates the effects of other components of W_c, which results in a decrease in W_c with k. In contrast, when k is large, customers may need to wait a very long time for order accumulation and delivery, both of which increase with k. Therefore, under large customer demand, the customer's waiting time first decreases and then increases with k, as shown in Figure 6b.

5 Operational strategies

This section describes two objectives for OFD platform operation: minimizing customer total waiting time (W_c) and maximizing order throughput (q_t). The former describes the service experience on the customer's side and the latter characterizes how much customer demand can be served by the platform. We also investigate the Pareto-efficient curve, which reflects the outcome of our multi-objective optimization. On the Pareto-efficient curve, there is no better possible outcome for one objective without causing the other optimized objective to become worse. For brevity, hereafter we denote the optimal customer total waiting time as W_c^* and q_t^* for the optimal order throughput.

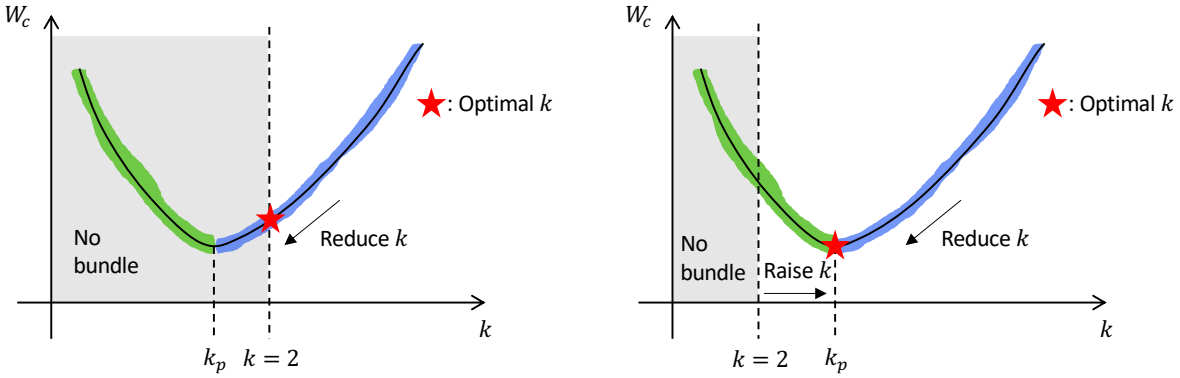

(a) Detrimental to increase k

(b) Beneficial to increase k for small k

Figure 6: Diagram for the insights of k; red stars are desired. k_p denotes that causes W_c to be the smallest.

5.1 Optimizing customer total waiting time

In this section, we discuss the tactical strategy for choosing a suitable pair of decision variables R and k to optimize customer total waiting time—i.e., to achieve the shortest customer total waiting time.

Proposition 3. *W_c^* always happens in the RP-SD scenario (including its boundaries, $\mathcal{L}_e \cap \{(R,k)|\Delta_c \leq 0\}$ and $\mathcal{L}_{RP,WP} \cap \{(R,k)|\Delta_c \leq 0\}$), where $W_{fp} = 0$ and $N_v \geq N_b$ (DSMR and RPWP criteria should be satisfied as described in Lemma 3 and Lemma 5).*

Proof. We find the shortest customer total waiting time using the diagram adapted from Figure 4, shown in Figure 7a. Note that the "Invalid region" refers to the scenario where $\theta > \pi$, which is outside the focus of this study (see discussion in Section 3.3.3). *Path 1* locates where R only cause the system to be SD scenario (below V_c), but drivers can either wait for food preparation or not. *Path 2* and *Path 3* are in the region where drivers have to wait for food preparation, but both SD and DD scenarios are possible. We then show that the customer total waiting time will decrease along each of these paths.

Along *Path 1* and according to our results for W_c in Table 2 and Table 3, we know that reducing the bundling ratio from an initial point in the region of the WP-SD scenario can reduce W_c, and thus improve W_c. Since it is possible for customer total waiting time in the RP-SD scenario to increase with k, the smallest W_c on *Path 1* will happen either at point V_1, or inside the region of the RP-SD scenario (W_c is continuous across $\mathcal{L}_{RP,WP}$ because the model solution is continuous according to Lemma 2). Along *Path 2* and according to our results for W_c in Table 3 and Table 4 and the continuity according to Lemma 2, we know that the smallest W_c happens at the point at the stability boundary $\mathcal{L}_e$, shown as the brown star in Figure 7a. Along *Path 3*, we prove in Appendix M that on the boundary $\mathcal{L}_e$, W_c decreases with R and k. Therefore, the smallest W_c on *Path 3* is at point V_c. Consequently, W_c^* always happens inside the region of the RP-SD scenario (including its boundaries). Therefore, to seek the W_c^*, the platform should ensure that the number of vacant drivers in the market is larger than the order bundles, and avoid causing drivers to wait at the restaurant for food preparation—then find a proper pair of R and k in the region of the RP-SD scenario for W_c^*. □

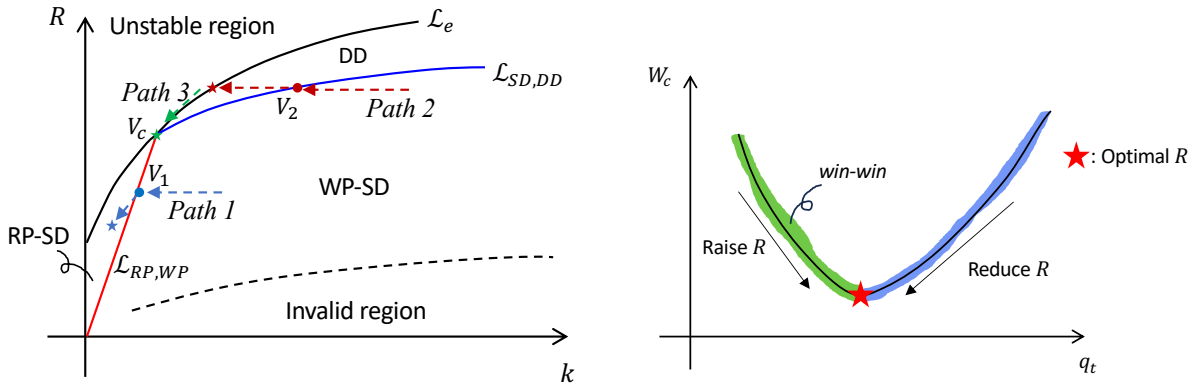

(a) Paths of decreasing W_c

(b) The win-win scenario of R (green)

Figure 7: Diagrams for Proposition 3 and Proposition 5.

5.2 Maximizing order throughput

Order throughput q_t is the quantity of customer demand that can be served by the system in a unit amount of time. If the system is stable, order throughput is equal to realized customer demand because all customer demand can be served. Otherwise, for a pair of decision variables (R, k) causing the system's being unstable because of insufficient delivery supply, order throughput is defined as the maximum rate of orders that can be served in which all the drivers are moving around for either delivery or return-pickup (where the order throughput is less than the customer demand). Thus, order throughput has two distinct formulations for the stable system and the unstable system:

$$q_t = \begin{cases} q, & \text{stable system,} \\ \hat{q} < q, & \text{unstable system.} \end{cases} \tag{36}$$

Proposition 4. *If the system does not meet the existence condition in Lemma 1, order throughput q_t equals $\hat{q}$, and it increases with k and decreases with R (see the specific expression of $\hat{q}$ in Appendix N).*

Proof. See Appendix N. □

Insight into R and k under an unstable system. If the system exhibits a shortage in delivery supply, the strategy of order bundling may effectively address this shortage. Consequently, an increase in variable k might facilitate system equilibrium. Moreover, a reduction in R is anticipated to decrease realized customer demand, and thereby further contribute positively to the stability of the system. Though order throughput can be defined in the unstable region, W_c is not defined when the system is unstable. This is because there will always be some customers in the system who cannot be served in an unstable system, and these customers' waiting time is undefined. According to Proposition 4, the platform operator should raise k or reduce R to reach the food delivery supply–demand balance again and avoid the system's instability.

For a stable system, q_t^* has the following property.

Proposition 5. *If the system meets the existence condition in Lemma 1, q_t^* happens when the maximum delivery distance is the largest possible. Also, since there exists a circumstance where R can reduce W_c according to Proposition 2.1, there exists a range of R that increasing R benefits both W_c and q_t. This is termed the win-win scenario, shown in Figure 7b.*

If the system meets the existence condition in Lemma 1, the rate of served customer demand is only related to maximum delivery distance R, and R contributes positively to q_t. This is because all realized customer demand will be served in the equilibrium state, and the larger the maximum delivery radius, the more customers will be covered and thus the larger q_t. Therefore, to seek q_t^*, platform operators should set the largest possible R provided that the solution exists as described in Lemma 1.

At this point, we know the tactical strategies for W_c minimization and q_t maximization, respectively: For W_c^*, the platform should control the decision variables so that the system falls into the RP-SD scenario; for q_t^*, the platform should increase the maximum delivery distance. For both objectives, to ensure that the system reaches equilibrium, the bundling ratio should be larger than the bundling threshold $k > k_c$. If the system falls into an unstable region, increasing k or decreasing R can help the system achieve the food delivery supply–demand balance again. However, the two optimization objectives contradict each other. q_t^* features the largest possible R—but W_c^* lies inside the decision space of the RP-SD scenario, which normally does not guarantee q_t^*. Therefore, decision-makers should refer to the Pareto-efficient curve, which can guide them for the bi-objective operations.

5.3 Bi-objective optimization and the Pareto-efficient curve

The tactical strategy guided by two objectives varies from the relative importance of each objective. Therefore, we investigate the Pareto-efficient curve, which is the path of the transition from one extreme of solely optimizing W_c to another extreme of solely optimizing q_t. The optimal tactical strategy is obtained by solving the subsequent optimization problem:

$$\underset{k,R,N_b,N_v}{\text{maximize}} \quad \text{objective} = (1-w)\left(-W_c(k,R)\right) + wq_t(k,R) \tag{37a}$$

$$\text{s.t.} \quad \text{Equations (5) to (7), (12), (13), (16) to (18) and (23),} \tag{37b}$$

$$N_b \geq \lambda\tau, N_v \geq \lambda\tau, \tag{37c}$$

$$\pi \geq \theta, \frac{1}{\tau_M} \geq \frac{q}{M}, \tag{37d}$$

where the two objectives are combined by the weighted sum strategy (Coleman et al., 1999, pp, 2–35), and $0 \leq w \leq 1$ is the weighting coefficient. The optimal value of Equation (37d) is W_c^* when $w = 0$, and is q_t^* when $w = 1$. Denoting the optimal solution of Equation (37d) as (R^*, k^*), we can express them as a function of w: $(R^*, k^*) = [R^*(w), k^*(w)]$. For different weighting factors w the optimal solution differs, and therefore all of the solutions can form a continuous path in the decision space $\mathcal{S}$, which is the Pareto-efficient curve $\mathcal{L}_{Pareto} = \{[R^*(w), k^*(w)] | 0 \leq w \leq 1\}$. However, solving the optimization problem in Equation (37d) is analytically intractable, we then demonstrate the Pareto curve in the numerical study and identify the optimal tactical strategies. The weighted sum strategy can produce the Pareto curve only if the curve lies on the convex boundary of the stable region (in the objective space). We thus need to validate this prerequisite in our numerical experiments.

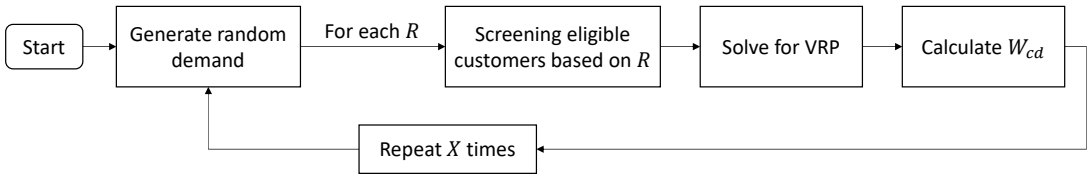

Figure 8: Simulation logic

6 Numerical study

This section validates our analytical findings using simulation and numerical demonstrations. We first conduct a Monte Carlo simulation using a less restrictive setting and then illustrate the system numerically using different pairs of (R, k) under different setting of exogenous variables. Both the simulation study and the numerical demonstration validate the key analytical findings in this study.

6.1 Monte Carlo simulation on driver routing

The simulation is designed in a less restrictive setting where drivers' routings are specifically relying on randomly distributed customer demand rather than a predetermined approximated route. It verifies one of the key analytical findings of this paper, i.e., the non-monotonic response of delivery time with respect to the maximum delivery distance. The simulation outcomes align with our analytical results which demonstrates the robustness of our findings and also the usage of continuum approximation in driver routing.

The simulation logic is shown in Figure 8 as follows. For every pair of (R, k), we first generate a cluster of random customer demand around a merchant and then screen eligible customers based on the maximum delivery distances, and solve a vehicle routing problem (VRP) for the eligible customers. Finally, we calculate each customer's delivery time. This process is repeated X times where X is a large enough number (here, we use $X = 100$). Therefore, for every pair of (R, k) we will have an average customer delivery time. To discover how R and k would impact on $W_{c,d}$, we run the simulation for different pairs of decision variables. Note that, the simulation exhibits huge stochasticity and to see the trend of $W_{c,d}$ with respect to R, we offset those $W_{c,d}$ under large R using the $W_{c,d}$ under the smallest R, and draw the curve of $W_{c,d}$'s v.s. R's. For example, if the smallest R in the trial set is $R = 2$ km and we have its associated delivery time $W_{cd,R=2}$, then for $R = 3$ km we also have $W_{cd,R=3}$, and so do later R's. Then on the graph, we show $\{0, W_{cd,R=3} - W_{cd,R=2}, W_{cd,R=4} - W_{cd,R=2}, \cdots\}$ v.s. $\{2, 3, 4, \cdots\}$. Additionally, we also present the subtraction set $\{W_{cd,R=R_i} - W_{cd,R=R_{i-1}}\}$ with respect to $\{R_i\}$. Therefore, to validate the non-monotonicity of $W_{c,d}$ with R, we need to show in the trend graph a non-monotonic curve, and equivalently, to show negative mean values of subtraction values in the subtraction curve. Figures 9 to 11 show the simulation results. It is validated that as R increases, the trend of delivery time holds a non-monotonic relationship with R. Also, they show that as demand increases, the minimum value of delivery time decreases, which aligns with our analytical analysis (i.e., Equation (79)).

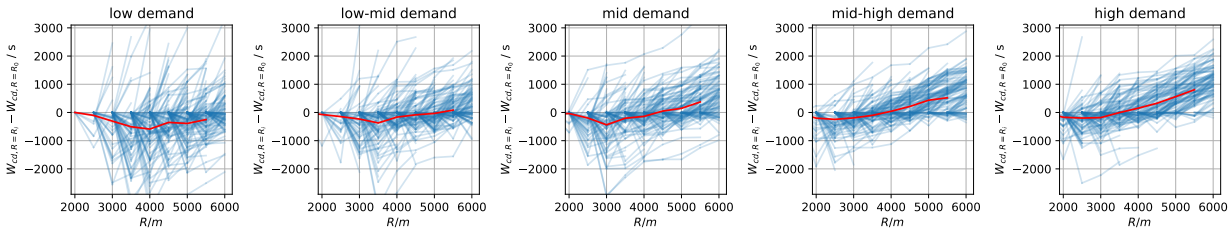

(a) Curves of $W_{cd,R=R_i} - W_{cd,R=R_0}$ with R. Blue curves: simulation results; red curve: mean.

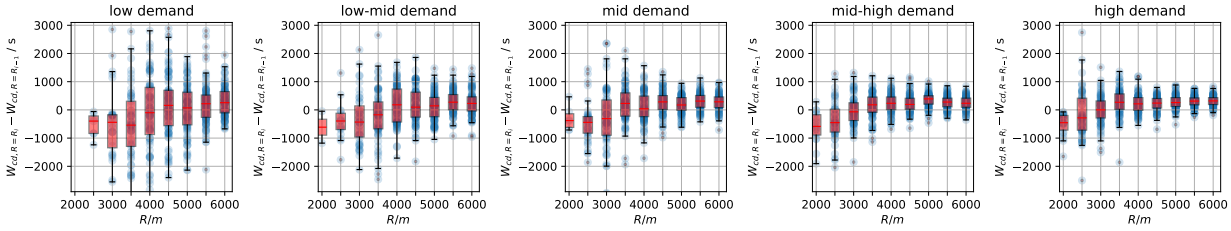

(b) Boxplot of $W_{cd,R=R_i} - W_{cd,R=R_{i-1}}$ with R. Blue dots: simulation results; red boxes: boxplot.

Figure 9: Simulation results of $k = 5$

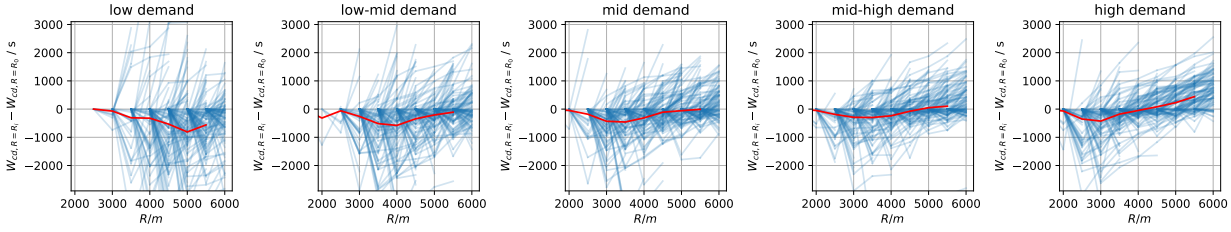

(a) Curves of $W_{cd,R=R_i} - W_{cd,R=R_0}$ with R. Blue curves: simulation results; red curve: mean.

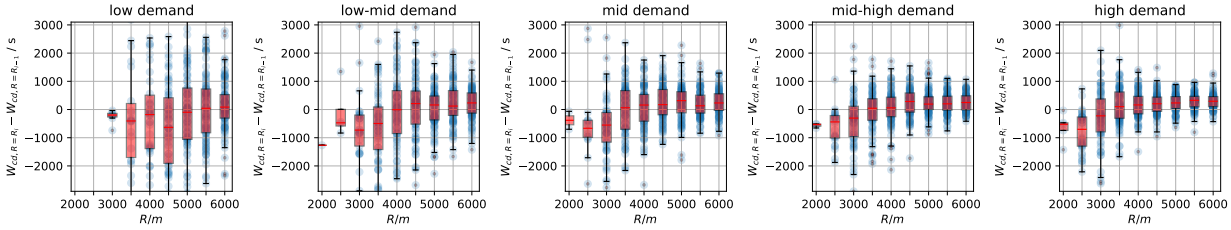

(b) Boxplot of $W_{cd,R=R_i} - W_{cd,R=R_{i-1}}$ with R. Blue dots: simulation results; red boxes: boxplot.

Figure 10: Simulation results of $k = 7$

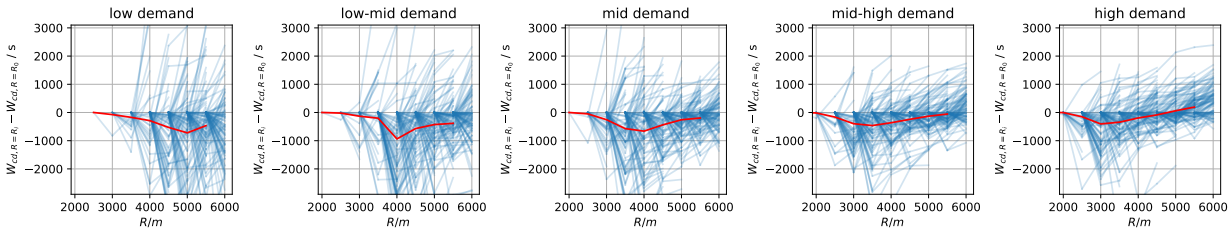

(a) Curves of $W_{cd,R=R_i} - W_{cd,R=R_0}$ with R. Blue curves: simulation results; red curve: mean.

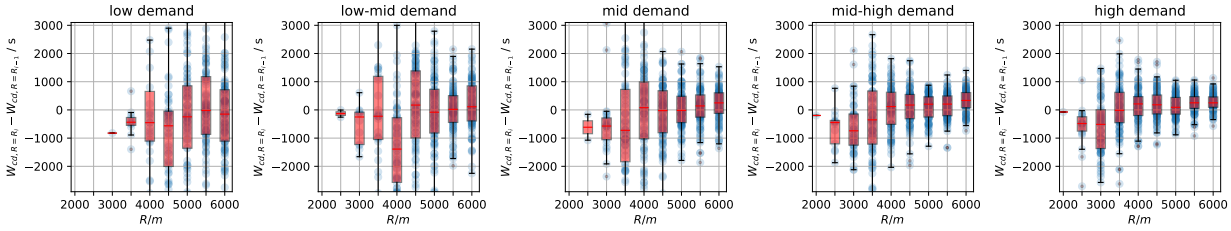

(b) Boxplot of $W_{cd,R=R_i} - W_{cd,R=R_{i-1}}$ with R. Blue dots: simulation results; red boxes: boxplot.

Figure 11: Simulation results of $k = 9$

6.2 Numerical demonstration of properties

In this section, we perform numerical experiments to show our managerial findings and tactical strategies. We consider two experimental settings presented in Table 5. Setting 1 presents a case in which customer demand per merchant is low (2 orders/hr), while the customer demand per merchant in Setting 2 is relatively higher (20 orders/hr). This difference in demand effectively demonstrates the different properties of the model under low or high customer demand rates. Also, the restaurant's food preparation rate in Setting 1 is lower, which facilitates a clearer observation of the DD scenario in this context. The value choices of parameters used in Table 5 are motivated by values reported in a research study by Meituan, a leading online food delivery (OFD) platform. For example, according to Meituan Research Institute and China Hotel Association (2019), the number of daily active drivers in Meituan in the first three quarters of 2019 is around 750 thousand and the total number of daily order transactions is around 26.8 million. Considering a Chinese fourth-tier city (e.g., Shaoguan city, around 2.8 million population) which takes the share of the OFD market of 0.12% (90 fourth-tier cities collectively share 10.9% of the market), there are around 3000 transactions every hour. Similarly, the average hourly transaction for a fifth-tier city is around

Table 5: Numerical experiment settings

Parameters	Setting 1	Setting 2
τ [hr]	0.005	0.005
$\overline{q}$ [orders/hr]	1000	3000
M [restaurants]	500	50
N [vehicles]	600	600
v [km/hr]	7	20
$1/\tau_M$ [orders/hr]	2	60

1000. Considering drivers' working time, there should be less than 900 active drivers every hour and thus we use a fleet size of 600. However, we acknowledge that certain parameters, such as those related to specific operational characteristics or cost structures, are challenging to obtain due to the proprietary nature of platform data and the lack of comprehensive public reports. To address this, we used synthetic data for parameters where real-world values are unavailable. These synthetic values were chosen to reflect reasonable ranges based on our understanding of OFD systems and to ensure the internal consistency of the model. For example, we use an average driver speed of 7 km/hour and 20 km/hour representing those who ride bikes or e-bikes/motorcycles, respectively, for delivery in urban areas, and we use the food preparation rate ($1/\tau_M$) of 2 orders/hour for the slow case (Setting 1) and 60 orders/hour for a fast case (Setting 2), etc.

It is worth noting that the primary purpose of the numerical study is to illustrate and validate the analytical findings, rather than to conduct a comparative study. Specifically, the numerical experiments are designed to demonstrate the existence and behavior of the insights derived from our theoretical framework. The values chosen in the numerical experiments are intended to highlight the correctness of the findings across different scenarios. Next, we first show how the three scenarios are distributed in $\mathcal{S}$ in the R-k coordinate system in Figure 12, and then present their model properties in Figure 13 and Figure 14, respectively. Finally, we show the Pareto-efficient curve for both settings in Figure 15.

Figure 12 depicts a scenario in which all of the RP-SD scenario, WP-SD scenario, and DD scenario exist. As shown, stable regions for the RP-SD scenario, WP-SD scenario, and DD scenario are mutually exclusive, and the unstable region locates in the top-left corner of the coordinates. This indicates that large R or small k will cause the system to be unstable, consistent with our discussion of Proposition 1.

We also show contour maps of customer total waiting time and order throughput q_t in Figure 13. According to the contours Figure 13a, the minimum W_c locates in the decision space of the RP-

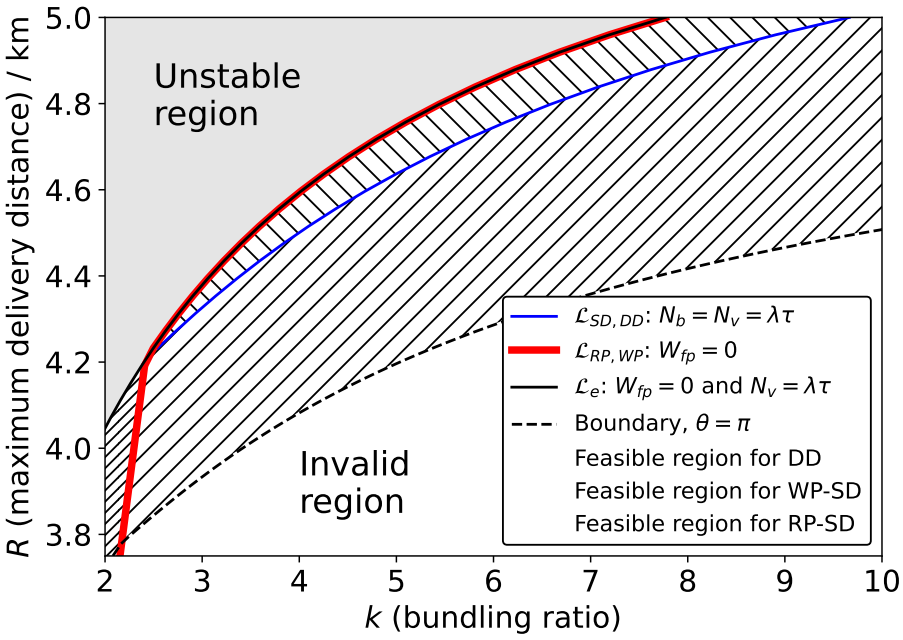

Figure 12: A sample decision plane in which all 3 scenarios are presented (experimental setting 1)

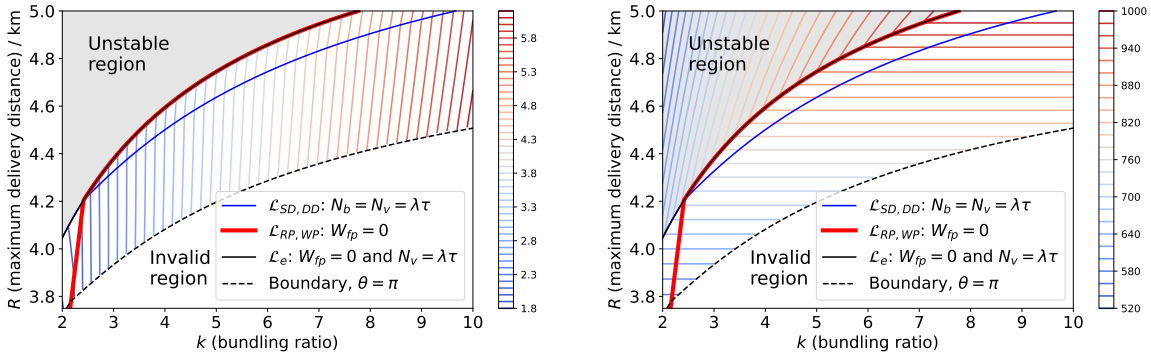

(a) Contours of W_c **(b)** Contours of q_t

Figure 13: Numerical experiment for Proposition 1, Proposition 3, and Proposition 5 (experimental setting 1)

SD scenario (the top-left corner of the RP-SD scenario), which validates Proposition 3. For q_t maximization in Figure 13b, the larget order throughput is at the top boundary of the coordinates, which is consistent with our proposed strategy: Choose the largest R in the stable region in Proposition 5. In the unstable region, W_c is undefined and order throughput increases with k and decreases with R, which validates Proposition 4.

Figure 14 depicts a different market exogenous variable setting with an emphasis on the SD scenario. The non-monotonic properties of customer accumulation time, delivery time, and total waiting time with respect to R are clearly shown. As can be seen in Figure 14a and Figure 14b, there exists a first decreasing, then increasing, relationship of accumulation time and delivery time with respect to the maximum delivery distance R. Also, there exists a non-monotonic relationship of W_c with R and k in Figure 14c, which shows the desire for order bundling at high demand (large R) but not under low demand (small R). These phenomena align with our analytical findings presented in Proposition 2.

As shown in Figure 14c, there is a region (for example, when $R = 4$ km) in which the W_c curve is not monotonic with respect to k. This corresponds to the scenario we discussed in Proposition 2.3, in which decision-makers should increase k when it is low and decrease k when it is high. It is also easy to observe the win-win scenario in which an increase in R will benefit both W_c and q_t (for instance, when $k = 2$ in Figure 14c and Figure 14d). However, the optimal point of W_c is obviously not the optimum of q_t, and then the Pareto-efficient curve is beneficial for platform operators seeking to make decisions based on their targets, which is presented in Figure 15.

Remark 1. *When the objective changes from W_c to q_t, i.e., when w changes from 0 to 1, both the optimal bundling ratio k^* and the optimal maximum delivery distance R^* increase.*

Figure 15 presents Pareto-efficient curves for the bi-objective optimization problem in both the R-k decision space and the W_c-q_t objective space. As shown in Figure 15a and Figure 15c, q_t^* happens at the top boundary of the coordinates and the optimal point for maximizing W_c lies in the decision space in the RP-SD scenario. The Pareto curve shows the optimal choice of decision variables for different weights of q_t and W_c. If decision-makers regard W_c as more important, they may choose a pair of decision variables close to the red star, which lies inside the decision space of the RP-SD scenario, and close to the green star if they think raising q_t is more important. In the objective space, we can see that the Pareto frontiers lie in the boundaries of the space where

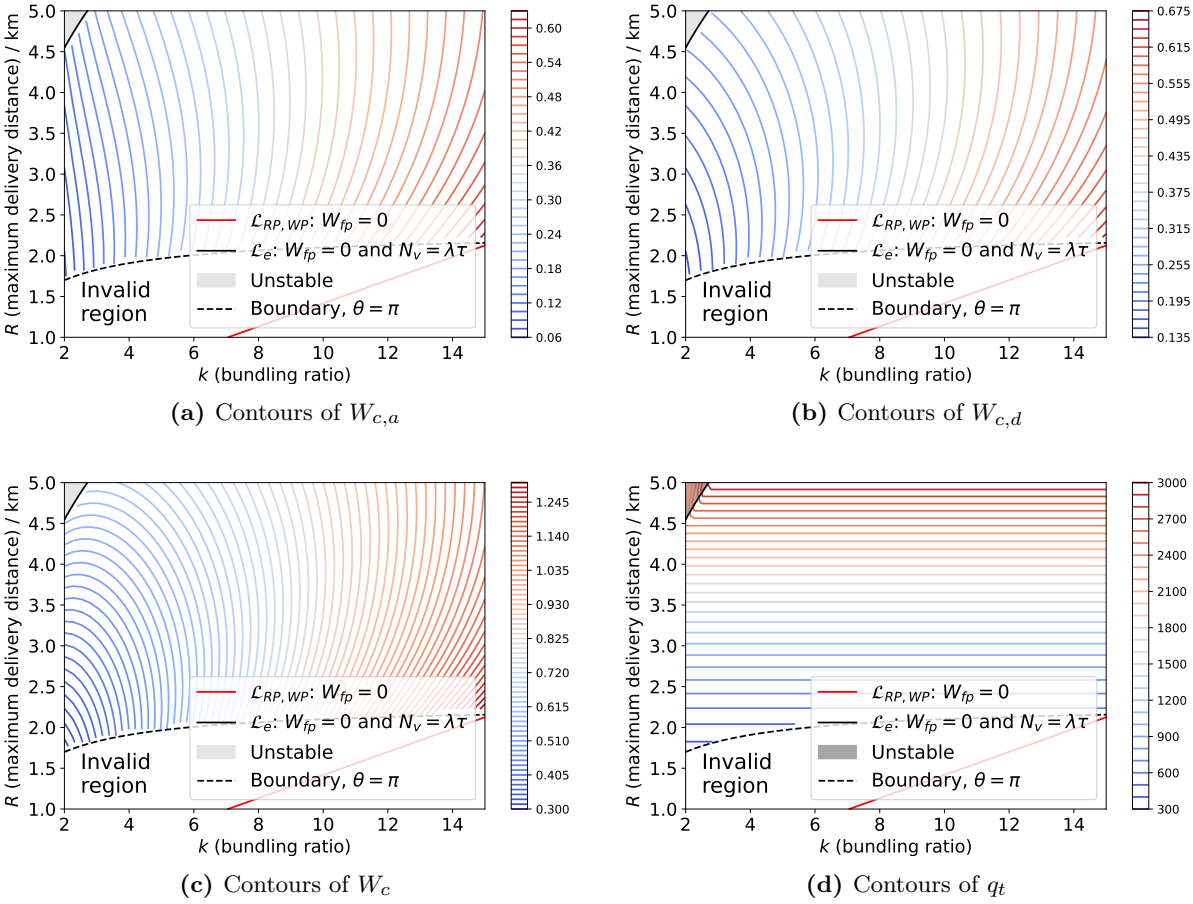

(a) Contours of $W_{c,a}$

(b) Contours of $W_{c,d}$

(c) Contours of W_c

(d) Contours of q_t

Figure 14: Numerical experiment for the properties of the decision variables in Proposition 2 (using experimental setting 2). "Over-saturated demand" (see Section 3.3.4) means that demand results in the restaurant's inability to prepare the meals.

the system is in equilibrium, which are convex frontiers; therefore, our use of the weighted sum strategy in Equation (37d) is adequate. From the Pareto curve, we also know that both optimal bundling ratio k^* and optimal maximum delivery distance R^* increase when the objective changes from W_c to q_t. The intuition is that when q_t is becoming more important, R should be set larger. When R increases, more customer demand is included in the system and it requires a larger k to reach an optimal operation to respond to the larger demand.

7 Conclusion

We use market equilibrium as a tool to develop an analytical model from a high-level perspective for on-demand food delivery (OFD) service that considers adjustable service region, order bundling, and batch-matching. Under market equilibrium of delivery supply and demand balance, i.e., the OFD demand is balanced with the delivery supply and the matching rate, we study the impact of two decision variables (R and k) in a good market condition (i.e., no excessively large or small demand), and provide various managerial insights, which we summarize as follows.

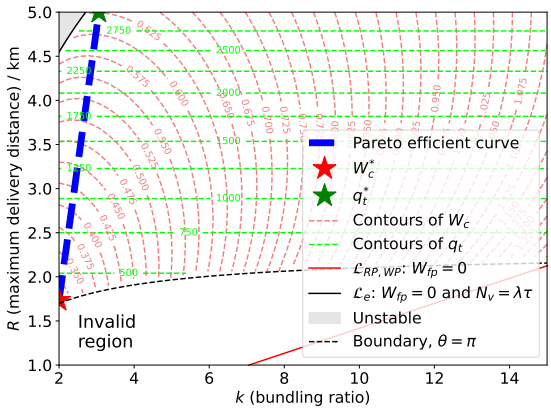

(a) Pareto curve for the setting of Figure 14 in the decision variable space

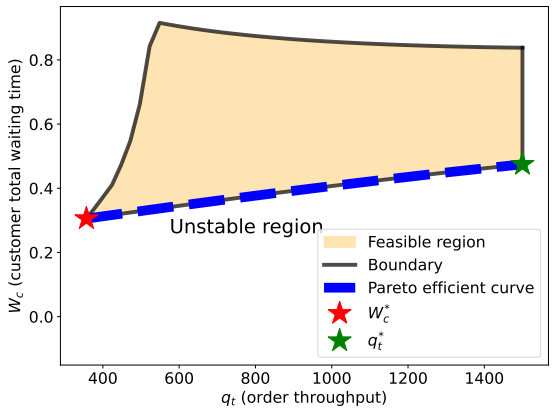

(b) Pareto curve for the setting of Figure 14 in the objective space

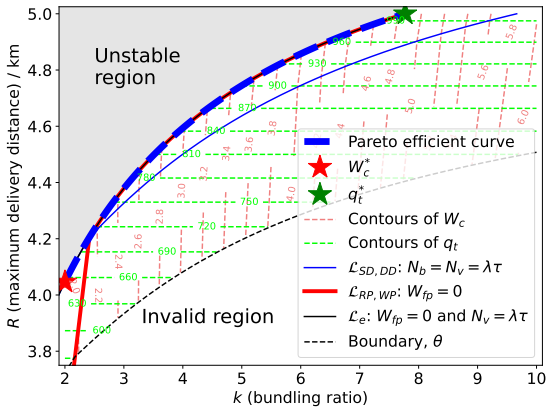

(c) Pareto curve for the setting of Figure 13 in the decision variable space

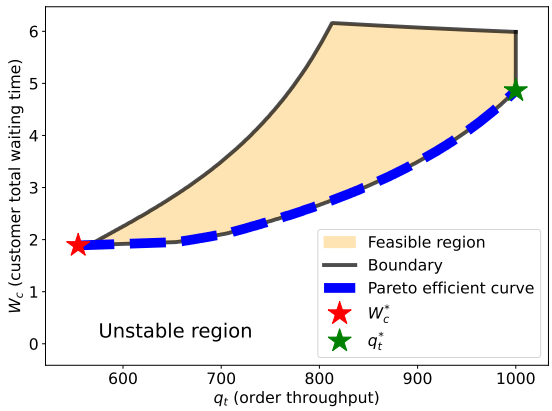

(d) Pareto curve for the setting of Figure 13 in the objective space

Figure 15: Illustration of the Pareto-efficient curves (thick dashed blue curves), W_c^* (red stars), and q_t^* (green stars) in both the decision space and the objective space.

First, regarding the maximum delivery distance. In the supply-dominant scenario, delivery time first decreases and then increases with maximum delivery distance. This non-monotonic behavior is due to the different responses of the axial and transversal distances on the driver's delivery route. The conflicting change in axial and transversal sizes of the delivery area (a slice of a circular disk) also contributes to the non-monotonic relationship of customer accumulation time with R. Apart from those, R also affects customer total waiting time in a non-monotonic way because the customer total waiting time is majorly influenced by $W_{c,a}$ and $W_{c,d}$, both of which first decrease and then increase with R. Also, due to the non-monotonicity of R on W_c, there exists a win-win scenario in which raising R can benefit both W_c and order throughput q_t.

The second conclusion regards the bundling ratio. The decision of the bundling ratio depends on the volume of the customer demand rate. If the demand is excessively large, adopting order bundling and increasing the bundling ratio can enhance the system's delivery supply and ultimately help the system to maintain the delivery supply–demand balance. When demand is large, yet within a range that remains within the system's food delivery capacity, there is an optimal bundling ratio that minimizes customer total waiting time. In cases of low demand, bundling becomes unnecessary, since bundling itself leads to detours and additional order accumulation time, both of

which negatively impact the service quality.

We also design optimal strategies for minimizing customer total waiting time and maximizing order throughput. For q_t maximization, the maximum delivery distance R should be set as large as possible. However, to optimize W_c, optimal R and k are normally small, whereby the operators should ensure that the OFD system is under the RP-SD scenario. On the Pareto-efficient curve, we observe that for an increase in R^*, the optimal bundling ratio k^* also increases when transitioning from optimizing W_c to optimizing q_t.

We acknowledge that the proposed model has some limitations. First, our model focuses on investigating the high-level impacts of the decision variables, and thus we did not consider the spatial and temporal dynamics of orders. Second, our findings are based on the approximation of customer arrivals through a fluid model, in which queue length's response in the food preparation period to increased demand is neglected. Also, our approximation on delivery route is for the average behavior of the driver route which might not align with the single driver behavior in the real world. However, these approximations are made to maintain analytical tractability and fair comparison among drivers, which are particularly useful for deriving closed-form solutions and provide theoretical guarantees for managerial insights. Third, this study adopts a series of simplifications and assumptions to ensure analytical tractability. While these simplifications inevitably abstract certain aspects of real-world complexity, they are carefully chosen to retain the most critical features of the market within the model. For example, demand is represented as a function of R, which, despite its simplicity, captures the core behavior of demand as influenced by delivery range. This formulation not only preserves the essential characteristics of customer behavior in the market but also facilitates the derivation of insightful analytical results regarding the impact of R on system performance. Future studies could build on this framework by relaxing some of these assumptions to incorporate additional real-world complexities. Additionally, future research is promising if more data is available. This study has the potential to be improved by calibrating its parameters such as η, and performing a more accurate numerical study (both simulation and numerical demonstration calibration). Besides, the demand generation process and the relationship between dining demand and OFD-enabled trip demand could be explicitly studied. This can also be done by building a network-level model and integrating the dining demand generation process into the network model. The induced trip and its impact on the entire road network could be analyzed in the network scope.

The abovementioned limitations fall into other aspects of the OFD market and will require more specific models, and these aspects are left to be investigated in future studies. This work is one of the first attempts to investigate the tactical strategies of systematically deciding the service region size and bundling ratio for the OFD market under batch matching, and we hope our work can motivate further research on the OFD system.

Acknowledgments

Kaihang Zhang would like to acknowledge the support from the Hong Kong PhD Fellowship Scheme; Jintao Ke would like to acknowledge support from the Hong Kong Research Grants Council under Early Career Scheme Project No. HKU27203323; Hai Wang would like to acknowledge support from the Lee Kong Chian Fellowship awarded by Singapore Management University; Yafeng Yin would like to acknowledge support from US National Science Foundation (CMMI-1854684).

Declaration of generative AI and AI-assisted technologies

During the preparation of this work the authors used generative AI tools to improve language and readability of some parts of this work. After using this tool/service, the authors reviewed and edited the content as needed and took full responsibility for the content of the publication.

References

Agatz, N., Cho, S.-H., Sun, H., & Wang, H. (2024). Transportation-enabled services: Concept, framework, and research opportunities. *Service Science*, *16*(1), 1–21. https://doi.org/10.1287/serv.2024.0116

Bahrami, S., Nourinejad, M., Yin, Y., & Wang, H. (2023). The three-sided market of on-demand delivery. *Transportation Research Part E: Logistics and Transportation Review*, *179*, 103313. https://doi.org/10.1016/j.tre.2023.103313

Baron, O., Chen, X., & Li, Y. (2023). Omnichannel services: The false premise and operational remedies. *Management Science*, *69*(2), 865–884. https://doi.org/10.1287/mnsc.2022.4416

Behrendt, A., Savelsbergh, M., & Wang, H. (2023). A prescriptive machine learning method for courier scheduling on crowdsourced delivery platforms. *Transportation Science*, *57*(4), 889–907. https://doi.org/10.1287/trsc.2022.1152

Benjaafar, S., Wu, S., Liu, H., & Gunnarsson, E. B. (2022). Dimensioning on-demand vehicle sharing systems. *Management Science*, *68*(2), 1218–1232. https://doi.org/10.1287/mnsc.2021.3957

Carlsson, J. G., Liu, S., Salari, N., & Yu, H. (2024). Provably good region partitioning for on-time last-mile delivery. *Operations Research*, *72*(1), 91–109. https://doi.org/https://doi.org/10.1287/opre.2021.0588

Chen, M., Hu, M., & Wang, J. (2022). Food delivery service and restaurant: Friend or foe? *Management Science*, *68*, 6539–6551. https://doi.org/10.1287/mnsc.2021.4245

Chen, Y., & Wang, H. (2018). Pricing for a last-mile transportation system. *Transportation Research Part B: Methodological*, *107*, 57–69. https://doi.org/10.1016/j.trb.2017.11.008

Coleman, T., Branch, M. A., & Grace, A. (1999). *Optimization toolbox user's guide* (2nd ed.). The MathWorks, Inc.

Jabali, O., Gendreau, M., & Laporte, G. (2012). A continuous approximation model for the fleet composition problem. *Transportation Research Part B: Methodological*, *46*(10), 1591–1606. https://doi.org/10.1016/j.trb.2012.06.004

Ke, J., Wang, C., Li, X., Tian, Q., & Huang, H.-J. (2024). Equilibrium analysis for on-demand food delivery markets. *Transportation Research Part E: Logistics and Transportation Review*, *184*, 103467. https://doi.org/10.1016/j.tre.2024.103467

Li, C., Mirosa, M., & Bremer, P. (2020). Review of online food delivery platforms and their impacts on sustainability. *Sustainability*, *12*(14), 5528. https://doi.org/10.3390/su12145528

Li, X., Ke, J., Yang, H., Wang, H., & Zhou, Y. (2024). An aggregate matching and pick-up model for mobility-on-demand services. *Transportation Research Part B: Methodological*, *190*, 103070. https://doi.org/10.1016/j.trb.2024.103070

Liang, J., Ke, J., Wang, H., Ye, H., & Tang, J. (2023). A poisson-based distribution learning framework for short-term prediction of food delivery demand ranges. *IEEE Transactions on Intelligent Transportation Systems*, 1–14. https://doi.org/10.1109/TITS.2023.3297948

Liang, J., Zhao, Y., Wang, H., Xiao, Z., & Ke, J. (2024). Uncovering merchants' willingness to wait in on-demand food delivery markets. *Transport Policy*, *158*, 14–28. https://doi.org/10.1016/j.tranpol.2024.09.002

Liu, S., He, L., & Shen, M. Z.-J. (2021). On-time last-mile delivery: Order assignment with travel-time predictors. *Management Science*, *67*(7), 4095–4119. https://doi.org/10.1287/mnsc.2020.3741

Mao, W., Ming, L., Rong, Y., Tang, C. S., & Zheng, H. (2019). Faster deliveries and smarter order assignments for an on-demand meal delivery platform. (ssrn. 3469015). https://doi.org/10.2139/ssrn.3469015

Mao, W., Ming, L., Rong, Y., Tang, C. S., & Zheng, H. (2022). On-demand meal delivery platforms: Operational level data and research opportunities. *Manufacturing & Service Operations Management*, *24*(5), 2535–2542. https://doi.org/10.1287/msom.2022.1112

Meituan Research Institute & China Hotel Association. (2019). *Chinese take-out industry survey report (first three quarters of 2019)*. https://mri.meituan.com/research/report

Newell, G. F., & Daganzo, C. F. (1986). Design of multiple-vehicle delivery tours—I a ring-radial network. *Transportation Research Part B: Methodological*, *20*(5), 345–363. https://doi.org/10.1016/0191-2615(86)90008-1

Nguyen-Phuoc, D. Q., Nguyen, N. A. N., Nguyen, M. H., Nguyen, L. N. T., & Oviedo-Trespalacios, O. (2022). Factors influencing road safety compliance among food delivery riders: An extension of the job demands-resources (jd-r) model. *Transportation Research Part A: Policy and Practice*, *166*, 541–556. https://doi.org/10.1016/j.tra.2022.11.002

Reyes, D., Erera, A., Savelsbergh, M., Sahasrabudhe, S., & O'Neil, R. (2018). The meal delivery routing problem. *Optimization online*, *6571*.

Shortie, J. F., Thompson, J. M., Gross, D., & Harris, C. M. (2018). *Fundamentals of queueing theory* (5th ed.). Wiley.

Simoni, M. D., & Winkenbach, M. (2023). Crowdsourced on-demand food delivery: An order batching and assignment algorithm. *Transportation Research Part C: Emerging Technologies*, *149*, 104055. https://doi.org/10.1016/j.trc.2023.104055

The Business Research Company. (2023). *Online food delivery services global market report 2023*. https://www.researchandmarkets.com/reports/5735323/online-food-delivery-services-global-market-report?utm_source=BW%5C&utm_medium=PressRelease%5C&utm_code=m4hc4t%5C&utm_campaign=1715370+-+Global+Online+Food+Delivery+Services+Markets+2022-2026+%5C%26+2031+with+takeaway.com%5C%3b+Doordash%5C%3b+Deliveroo%5C%3b+Uber+eats%5C%3b+Zomato+Dominating&utm_exec=chdo54prd

Uber Technologies Inc. (2025). https://help.uber.com/en/merchants-and-restaurants/article/how-do-delivery-zones-work?nodeId=d27ee1ee-6c10-4aa4-bf11-54f0566e1392

Wang, H. (2022). Transportation-enabled urban services: A brief discussion. *Multimodal Transportation*, *1*(2), 100007. https://doi.org/10.1016/j.multra.2022.100007

Wang, H., & Odoni, A. (2016). Approximating the performance of a "last mile" transportation system. *Transportation Science*, *50*(2), 659–675. https://doi.org/10.1287/trsc.2014.0553

Wang, H., & Yang, H. (2019). Ridesourcing systems: A framework and review. *Transportation Research Part B: Methodological*, *129*, 122–155. https://doi.org/10.1016/j.trb.2019.07.009

Yang, H., Leung, C. W., Wong, S., & Bell, M. G. (2010). Equilibria of bilateral taxi–customer searching and meeting on networks [149 citations (Crossref) [2023-04-04]]. *Transportation Research Part B: Methodological*, *44*(8–9), 1067–1083. https://doi.org/10.1016/j.trb.2009.12.010

Yang, H., Qin, X., Ke, J., & Ye, J. (2020). Optimizing matching time interval and matching radius in on-demand ride-sourcing markets. *Transportation Research Part B: Methodological*, *131*, 84–105. https://doi.org/10.1016/j.trb.2019.11.005

Yang, H., & Yang, T. (2011). Equilibrium properties of taxi markets with search frictions. *Transportation Research Part B: Methodological*, *45*(4), 696–713. https://doi.org/10.1016/j.trb.2011.01.002

Yang, J., Lau, H. C., & Wang, H. (2024). Optimization of customer service and driver dispatch areas for on-demand food delivery. *Transportation Research Part C: Emerging Technologies*, *165*, 104653. https://doi.org/10.1016/j.trc.2024.104653

Ye, A., Zhang, K., Bell, M. G., Chen, X., & Hu, S. (2024a). Modeling an on-demand meal delivery system with human couriers and autonomous vehicles in a spatial market. *Transportation Research Part C: Emerging Technologies*, 104723. https://doi.org/10.1016/j.trc.2024.104723

Ye, A., Zhang, K., Chen, X., Bell, M. G., Lee, D.-H., & Hu, S. (2024b). Modeling and managing an on-demand meal delivery system with order bundling. *Transportation Research Part E: Logistics and Transportation Review*, *187*, 103597. https://doi.org/10.1016/j.tre.2024.103597

Yildiz, B., & Savelsbergh, M. (2019a). Service and capacity planning in crowd-sourced delivery. *Transportation Research Part C: Emerging Technologies*, *100*, 177–199. https://doi.org/10.1016/j.trc.2019.01.021

Yildiz, B., & Savelsbergh, M. (2019b). Provably high-quality solutions for the meal delivery routing problem. *Transportation Science*, *53*(5), 1372–1388. https://doi.org/10.1287/trsc.2018.0887

Zha, L., Yin, Y., & Xu, Z. (2018). Geometric matching and spatial pricing in ride-sourcing markets. *Transportation Research Part C: Emerging Technologies*, *92*, 58–75. https://doi.org/10.1016/j.trc.2018.04.015

Zhao, L., Wang, H., Yile, L., Li, D., Zhao, J., Ding, X., Hao, J., & He, R. (2024). *The first informs tsl data-driven research challenge (tsl-meituan 2024): Background and data description.* https://github.com/meituan/Meituan-INFORMS-TSL-Research-Challenge/tree/main

Zhou, Y., Yang, H., Ke, J., Wang, H., & Li, X. (2022). Competition and third-party platform-integration in ride-sourcing markets. *Transportation Research Part B: Methodological*, *159*, 76–103. https://doi.org/10.1016/j.trb.2021.08.002

Zhu, L., Yu, W., Zhou, K., Wang, X., Feng, W., Wang, P., Chen, N., & Lee, P. (2020). Order fulfillment cycle time estimation for on-demand food delivery. *Proceedings of the 26th ACM SIGKDD International Conference on Knowledge Discovery & Data Mining*, 2571–2580. https://doi.org/10.1145/3394486.3403307

Appendix A Proof of Equation (15)

$$
\begin{aligned}
W_{c,d} &= \frac{1}{vk}\left[\sum_{n:n\le k/2}(nL_p+(n-1)l_t)+\sum_{n:n>k/2}((n-1)L_p+nl_t)\right],\\
&= \frac{1}{vk}\left[\sum_{n:n\le k/2}nL_p+\sum_{n:n\le k/2}(n-1)l_t+\sum_{n:n>k/2}(n-1)L_p+\sum_{n:n>k/2}nl_t\right],\\
&= \frac{1}{vk}\left[-\frac{k}{2}L_p-\frac{k}{2}l_t+\sum_{n=1}^{k}nL_p+\sum_{n=1}^{k}nl_t\right],\\
&= \frac{1}{vk}\left[(L_p+l_t)\left(-\frac{k}{2}+\sum_{n=1}^{k}n\right)\right]=\frac{1}{vk}\left[\frac{k^2}{2}(L_p+l_t)\right]=\frac{L_p+L_d+2R(\eta-1)}{2v}.
\end{aligned}
$$

Appendix B Influence of the demand density rate

The demand density rate influences the monotonicity of delivery times because drivers are spread over the delivery area and each driver is in charge of a sector with an inner angle θ. This sector assignment is dependent on the number of customers inside each sector. If δ is highly concentrated in the center and is small in the outer region of the delivery area, when R increases, reduction in the transversal travel distance is marginal compared with elongation of the axial travel distance. Therefore, the delivery distance may monotonically increase with R.

We will next identify what kind of demand profile would cause this non-monotonicity. We make a blanket assumption that realized demand q is an increasing, continuous, and differentiable function with R—i.e., the larger the delivery area, the more customer demand. Demand density rate δ can take various forms, such as decreasing, among others. Therefore, it is reasonable to say that customers' delivery time will increase with R when R is large because in this case, the included customer demand is very large and would render each driver's individual delivery area very narrow. Then, to investigate whether the delivery time is non-monotonic, we can focus on whether delivery time would decrease with R when R is relatively small. Also, we only need to focus on supply-dominant case, since a small R (small demand) will normally cause $N_v > N_b$. First, we consider the derivative of $W_{c,d}$ with R. In the RP-SD scenario, we have

$$
\frac{\mathrm{d}W_{c,d}}{\mathrm{d}R}=\frac{\partial W_{c,d}}{\partial q}\frac{\mathrm{d}q}{\mathrm{d}R}+\frac{\partial W_{c,d}}{\partial R}, \tag{38}
$$

$$
=\frac{-2\pi^2M^2R^2\delta k^2v/q+\pi Mk^2v+9Rq+3\sqrt{2\pi MRk^2qv+9R^2q^2}}{6v\sqrt{2\pi MRk^2qv+9R^2q^2}}. \tag{39}
$$

In the WP-SD scenario, we have

$$
\frac{\mathrm{d}W_{c,d}}{\mathrm{d}R}=\frac{\partial W_{c,d}}{\partial q}\frac{\mathrm{d}q}{\mathrm{d}R}+\frac{\partial W_{c,d}}{\partial R_s}\frac{\mathrm{d}R_s}{\mathrm{d}R}+\frac{\partial W_{c,d}}{\partial R}, \tag{40}
$$

$$
=\frac{-2\pi^2M^2R^2\delta k^4v/q+\pi Mk^4v+9R_skq(k-\eta)+3(k-\eta)\sqrt{2\pi MRk^4qv+9R_s^2k^2q^2}}{6kv\sqrt{2\pi MRk^4qv+9R_s^2k^2q^2}}. \tag{41}
$$

If these derivatives are negative when R is small, delivery time decreases with R. If we discover the sign of these derivatives, we can focus on the numerators because the denominators are positive. Consider the limit of a small R. For the RP-SD scenario, it is

$$
\lim_{R\to0^+}numerator=\lim_{R\to0^+}(-2\pi^2M^2R^2\delta k^2v/q+\pi Mk^2v). \tag{42}
$$

For the WP-SD scenario, it is

$$
\lim_{R\to0^+}numerator=\lim_{R\to0^+}(-2\pi^2M^2R^2\delta k^4v/(q\tau_M)+\pi Mk^4v/\tau_M). \tag{43}
$$

The condition whereby these limits are zero is

$$2\pi MR^2\delta = q, \tag{44}$$

where $2\pi MR\delta = \dfrac{\mathrm{d}q}{\mathrm{d}R}$ according to Equation (3), which yields

$$\frac{\mathrm{d}q}{\mathrm{d}R}R = q. \tag{45}$$

The general solution of this ordinary differential equation is

$$q = cR, \tag{46}$$

where c is a constant, and the corresponding demand density rate is

$$\delta = \frac{1}{2\pi MR}\frac{\mathrm{d}q}{\mathrm{d}R}, \tag{47}$$

$$= \frac{c}{2\pi MR}. \tag{48}$$

This general solution indicates that when q is a proportional function of R, customers' delivery time tends to be independent of R when R is very small. In this case, customer demand density rate δ is an inversely proportional function of R, which means the customer demand is relatively more concentrated in the center compared with the constant customer demand we used in the main text. If customer demand density gets even more concentrated in the center, customers' delivery time will be monotonic for every R; e.g., Figure 16a. Otherwise, for a more amortized customer demand density, customers' delivery time will present a first decreasing, then increasing, relationship with R; see Figure 16b.

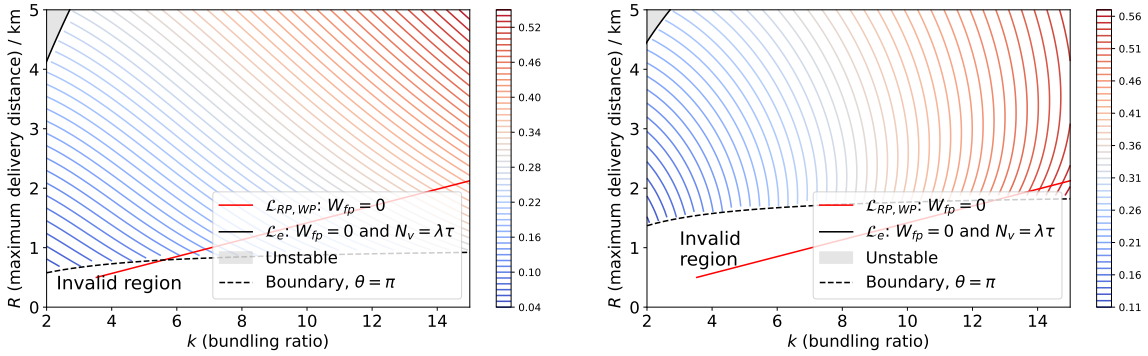

(a) Contours of $W_{c,d}$, $q = \overline{q}\left(\dfrac{R}{R_a}\right)^{0.5}$

(b) Contours of $W_{c,d}$, $q = \overline{q}\left(\dfrac{R}{R_a}\right)^{1.5}$

Figure 16: Contours of customers' delivery time for two different q profiles (using experimental setting 2).

Appendix C Simulation on driver routes

This section presents the results of our numerical experiments concerning the routes taken by drivers, in relation to open Vehicle Routing Problem (open-VRP) configurations. We executed Monte Carlo simulations, similar to the workflow as depicted in Figure 8, albeit within an open-VRP context instead of VRP. The aim was to validate whether the distance from the depot to the furthest delivery point exceeded the distance to the endpoint of each route.

The findings of these simulations are presented in Figure 17. These results confirm our hypothesis, confirming that the distance from the depot (in this case, the restaurant) to the most distant point on the delivery routes is, on average, shorter than the distance to the final drop-off location of the routes, and the result is statistically significant. This suggests that even within an open-VRP framework, drivers tend to return to the depot. The results also reflect that, a larger bundling ratio would result in a more return-like route. We also visualize some open-VRP results in Figure 18, which shows that the routes are similar to the VRP results.

It is important to note that this simulation did not factor in the potential influence of drivers' familiarity with specific regions. This familiarity could conceivably incline drivers further towards returning to the restaurant, given their preference for operating within known areas. Therefore, our findings suggest that the open-VRP delivery setting also commonly sees drivers returning to the depot and Figure 2 is applicable to represent the delivery route.

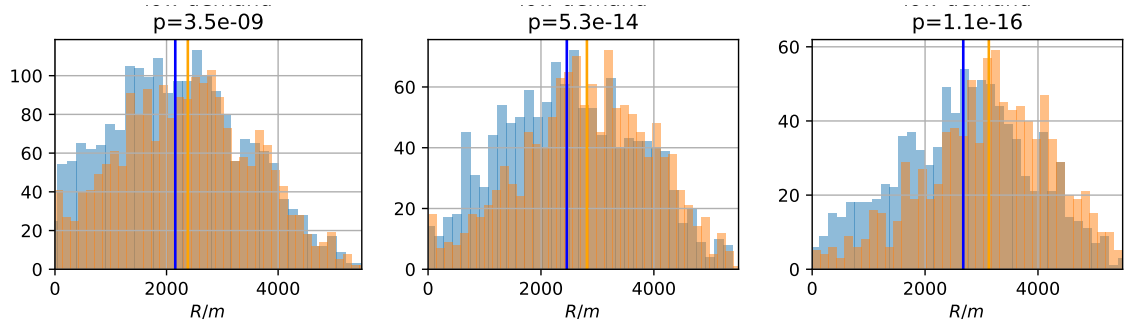

(a) $k = 5$ **(b)** $k = 7$ **(c)** $k = 9$

Figure 17: Distribution of the distance to endpoint (blue) and farthest point (orange) of routes where the p-value is drawn from the hypothesis test of whether the mean value of two distributions are different.

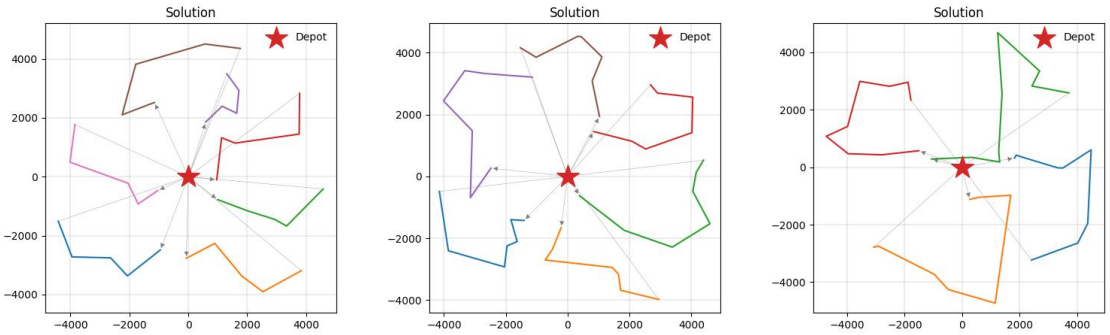

(a) $k = 5$ **(b)** $k = 7$ **(c)** $k = 9$

Figure 18: Visualization of some open-VRP results.

Appendix D Proof of Lemma 1

The stability of each scenario depends on whether food delivery supply can satisfy food delivery demand. To better understand the system, we introduce a concept called buffer driver, which includes drivers who are waiting for matching but will not get matched and those who are waiting for meal preparation (if it exists). Thus, $N_{buffer} = (N_v - \lambda\tau) + W_{fp}\lambda$. These two types of drivers can be regarded as a buffer in the system because when demand goes up, intuitively, these drivers can be assigned to order delivery or pickup, which can raise the system's food delivery supply and restore the system to equilibrium.

Thus, the critical condition for the system to be stable is that the number of buffer drivers equals 0. The critical bundling ratio can be calculated by substituting $W_{fp} = 0$ and $N_v = \lambda\tau$ into Equation (23), which gives

$$k_c = \frac{18NRq + 9Nq\tau v + 3q\sqrt{8\pi MR^2q\tau + 2\pi MRq\tau^2 v + 36N^2R^2}}{18N^2 v - 4\pi MRq}. \tag{49}$$

Therefore, if $k > k_c$ is met we have $N_{buffer} > 0$, and thus the food delivery supply is sufficient, which indicates that the equilibrium solution exists. Since this analysis is not differentiated from each scenario, the solution exists for all scenarios (defined in Section 4.1.1) as long as the existence condition is met. We also have $\mathrm{d}k_c/\mathrm{d}R > 0$, because

the numerator of k_c in Equation (49) increases with R but its denominator decreases with R. This trend can be interpreted as follows: If R increases, the critical bundling ratio should also increase to fulfill the increased demand.

Appendix E Proof of Lemma 2

We first prove that W_c is continuous at any point on $\mathcal{L}_{RP,WP}$.

Proof. Let (k_0, R_0) be a point on the curve $\mathcal{L}_{RP,WP} \subset \mathcal{S}$ and $\mathcal{N}_1$, $\mathcal{N}_2$ be the neighborhoods of (k_0, R_0) on either side of $\mathcal{L}_{RP,WP}$. For any pair of points (k_1, R_1) and (k_2, R_2) in $\mathcal{N}_1$ and $\mathcal{N}_2$, respectively, if we let (k_1, R_1) and (k_2, R_2) approach (k_0, R_0), and if the following condition is met:

$$\lim_{(k_1,R_1)\to(k_0,R_0)} (N_b, N_v) = \lim_{(k_2,R_2)\to(k_0,R_0)} (N_b, N_v), \tag{50}$$

W_c is continuous at any point on $\mathcal{L}_{RP,WP} \subset \mathcal{S}$. If $(k_1, R_1) \to (k_0, R_0)$ and $(k_2, R_2) \to (k_0, R_0)$, the equilibrium solution comes from Equation (23) with $W_{fp} = 0$, which certainly produces the same solution.

□

We then prove that W_c is continuous at any point on $\mathcal{L}_{SD,DD}$.

Proof. If the system is under the Wait-for-Pickup scenario according to the RPWP criterion in Lemma 5, let (k_a, R_a) be a point on the curve $\mathcal{L}_{SD,DD} \subset \mathcal{S}$ and $\mathcal{N}_b$, $\mathcal{N}_c$ be the neighborhoods of (k_a, R_a) on either side of $\mathcal{L}_{SD,DD}$. For any pair of points (k_b, R_b) and (k_c, R_c) in $\mathcal{N}_b$ and $\mathcal{N}_c$, respectively, if we let (k_b, R_b) and (k_c, R_c) approach (k_a, R_a), and if the following condition is met:

$$\lim_{(k_b,R_b)\to(k_a,R_a)} (N_b, N_v) = \lim_{(k_c,R_c)\to(k_a,R_a)} (N_b, N_v), \tag{51}$$

W_c is continuous at any point on $\mathcal{L}_{SD,DD} \subset \mathcal{S}$. If $(k_b, R_b) \to (k_a, R_a)$ and $(k_c, R_c) \to (k_a, R_a)$, the equilibrium solution comes from Equation (23) with $W_{c,q} = W_{v,q} = \tau/2$, which certainly produces the same solution.

□

Appendix F Proof of Lemma 3

From Equation (27) we have

$$8\pi MRk^2q - 36N^2k^2v + 72NR_skq + 36Nkq\tau v - 36R_sq^2\tau - 9q^2\tau^2v = 0, \tag{52}$$

where $R_s = R + W_{fp}v/2$ and the left-hand side of Equation (52) is defined as Δ_c. Since the solution is continuous on the curve $\mathcal{L}_{SD,DD}$ according to Lemma 2, we consider R_s using its formulation in the SD scenario, $R_s = \max\left[R + \frac{v}{2}\left(\tau_M - \frac{2R\eta}{kv} - \frac{\tau}{2}\right), R\right]$.

If the system is under certain decision variables such that $N_v = \hat{N}_v$, $N_b = \hat{N}_b$, and $\Delta_c = \hat{\Delta}_c \le 0$, simplify and reorder Equation (52). We have

$$\frac{2\pi MRq}{9v} - N^2 + 2NR_s\lambda/v + N\lambda\tau - R_s\lambda^2\tau/v - \frac{\lambda^2\tau^2}{4} \le 0, \tag{53}$$

$$\frac{1}{v}\left[\frac{2\pi MRk\lambda}{9\left(N - \frac{1}{2}\lambda\tau\right)} + 2R_s\lambda\right] + \frac{1}{2}\lambda\tau \le N, \tag{54}$$

$$\left[\lambda(W_p + W_{v,d} + W_{fp}) + N_v - \lambda\tau/2\right]\Big|_{N_v=N_b=\lambda\tau} \le N, \tag{55}$$

where the term $\left[\lambda(W_p + W_{v,d} + W_{fp}) + N_v - \lambda\tau/2\right]\Big|_{N_v=N_b=\lambda\tau}$ is equal to N if $\Delta_c = 0$. On top of that, it should be satisfied that $\lambda(W_p + W_{v,d} + W_{fp}) + N_v - \lambda\tau/2 = N, \forall(R,k)$. Since $\frac{\partial}{\partial N_b}(W_p + W_{v,d} + W_{fp}) \le 0$ and $\frac{\partial}{\partial N_v}(W_p + W_{v,d} + W_{fp}) > 0$, we also know from Section 3.4 that either N_b or N_v equals $\lambda\tau$. Therefore, the condition $\Delta_c \le 0$ (equivalently, Equation (55)) implies that $N_b = \lambda\tau, N_v \ge \lambda\tau$ or $N_b \le \lambda\tau, N_v = \lambda\tau$. Since both N_v and N_b should be greater than $\lambda\tau$, we have $N_b = \lambda\tau, N_v \ge \lambda\tau$, which indicates that the system is under the SD scenario. Conversely, if the system is under certain decision variables that have $\Delta_c = \hat{\Delta}_c > 0$, it is under the DD scenario.

Appendix G Proof of Lemma 4

Consider the implicit differentiation $\frac{\mathrm{d}R}{\mathrm{d}k}$ in Equation (52):

$$\frac{\mathrm{d}}{\mathrm{d}k}\left(8\pi MRk^2q-36N^2k^2v+72NR_skq+36Nkq\tau v-36R_sq^2\tau-9q^2\tau^2v\right)=0, \tag{56}$$

$$\begin{aligned}&16\pi MRkq+8\pi Mk^2\left(q\frac{\mathrm{d}R}{\mathrm{d}k}+\frac{\mathrm{d}q}{\mathrm{d}R}\frac{\mathrm{d}R}{\mathrm{d}k}R\right)-72N^2kv+72NR_sq\\&\quad+72Nk\left[q\left(\frac{\partial R_s}{\partial R}\frac{\mathrm{d}R}{\mathrm{d}k}+\frac{\partial R_s}{\partial k}\right)+R_s\frac{\mathrm{d}q}{\mathrm{d}R}\frac{\mathrm{d}R}{\mathrm{d}k}\right]+36N\tau vq+36Nk\tau v\frac{\mathrm{d}q}{\mathrm{d}R}\frac{\mathrm{d}R}{\mathrm{d}k}\\&\quad-36q^2\tau\left(\frac{\partial R_s}{\partial R}\frac{\mathrm{d}R}{\mathrm{d}k}+\frac{\partial R_s}{\partial k}\right)-36\tau R_s\cdot 2q\frac{\mathrm{d}q}{\mathrm{d}R}\frac{\mathrm{d}R}{\mathrm{d}k}-18q\tau^2v\frac{\mathrm{d}q}{\mathrm{d}R}\frac{\mathrm{d}R}{\mathrm{d}k}=0,\end{aligned} \tag{57}$$

where $\frac{\partial R_s}{\partial k}=\frac{R\eta}{k^2}$, and $\frac{\partial R_s}{\partial R}=-\frac{\eta}{k}+1$. Then we have

$$\frac{\mathrm{d}R}{\mathrm{d}k}=\frac{-16\pi MRkq+72N^2kv-72NR_sq-36Nq\tau v-72Nkq\frac{\partial R_s}{\partial k}+36q^2\tau\frac{\partial R_s}{\partial k}}{8\pi Mk^2\left(q+\frac{\mathrm{d}q}{\mathrm{d}R}R\right)+72Nk\left(q\frac{\partial R_s}{\partial R}+R_s\frac{\mathrm{d}q}{\mathrm{d}R}\right)+36Nk\tau v\frac{\mathrm{d}q}{\mathrm{d}R}-36q^2\tau\frac{\partial R_s}{\partial R}-72\tau R_sq\frac{\mathrm{d}q}{\mathrm{d}R}-18q\tau^2v\frac{\mathrm{d}q}{\mathrm{d}R}}, \tag{58}$$

$$=\frac{-16\pi MRkq+72N^2kv-72NR_sq-36Nq\tau v-\frac{72NqR\eta}{k}+\frac{36q^2\tau R\eta}{k^2}}{8\pi Mk^2\left(q+\frac{\mathrm{d}q}{\mathrm{d}R}R\right)+72Nk\left(q\frac{\partial R_s}{\partial R}+R_s\frac{\mathrm{d}q}{\mathrm{d}R}\right)+36Nk\tau v\frac{\mathrm{d}q}{\mathrm{d}R}-36q^2\tau\frac{\partial R_s}{\partial R}-72\tau R_sq\frac{\mathrm{d}q}{\mathrm{d}R}-18q\tau^2v\frac{\mathrm{d}q}{\mathrm{d}R}}. \tag{59}$$

Since the vehicle fleet size is larger than the number of drivers who are delivering, heading for pickup, and matching, we have (note that when $\Delta_c=0$, $N_b=N_v=\lambda\tau$)

$$N>\frac{q}{k}\left(\frac{2R_s}{v}+\frac{2Rk\theta}{9v}+\frac{\tau}{2}\right) \tag{60}$$

$$=\frac{q}{k}\left[\frac{2R_s}{v}+\frac{2\pi MRk}{9v(N-\lambda\tau/2)}+\frac{\tau}{2}\right]. \tag{61}$$

Multiplying the left-hand side by N yields

$$N^2>\frac{q}{k}\left[\frac{2R_s}{v}N+\frac{1}{2}N\tau+\frac{2\pi MRk}{9v}\frac{N}{N-\lambda\tau/2}\right] \tag{62}$$

$$>\frac{q}{k}\left[\frac{2R_s}{v}N+\frac{1}{2}N\tau+\frac{2\pi MRk}{9v}\right]. \tag{63}$$

Simplify, and we obtain

$$N^2kv>2NR_sq+\frac{1}{2}N\tau qv+\frac{2\pi MRkq}{9}. \tag{64}$$

Since the pickup distance is no larger than the maximum delivery distance, we have $\frac{2R\eta}{k}\le R$, which yields $\eta\le k/2<k$. Then the numerator of Equation (59) satisfies

$$\text{numerator of Equation (59)}>-16\pi MRkq+72N^2kv-72NR_sq-36Nq\tau v-\frac{72NqR\eta}{k} \tag{65}$$

$$>-16\pi MRkq+72N^2kv-72NR_sq-36Nq\tau v-72NqR \tag{66}$$

$$>-16\pi MRkq+72N^2kv-144NR_sq-36Nq\tau v, \tag{67}$$

which is greater than 0 because of Equation (64). Similarly, since $N>2\lambda R_s/v+\lambda\tau/2$ and $2Nk>q\tau$, the denominator of Equation (59) is also greater than 0. As a result, $\frac{\mathrm{d}R}{\mathrm{d}k}>0$.

Appendix H Proof of Lemma 5

In the SD scenario, if $\tau_M - \frac{2R\eta}{kv} - \frac{\tau}{2} \leq 0$, $W_{fp} = 0$, and thus the OFD system is under the RP scenario; if $\tau_M - \frac{2R\eta}{kv} - \frac{\tau}{2} > 0$, $W_{fp} > 0$ and the OFD system is under the WP scenario.

In the DD scenario, to ensure the solution exists, it should be satisfied that $W_{fp} \geq 0$ because $N_v = \lambda\tau$. When $W_{fp} = 0$, it corresponds to the RP scenario and the condition that $k = k_c(R)$, which means that the RP-DD scenario is on boundary $\mathcal{L}_e$. Otherwise, when $W_{fp} > 0$, it should be satisfied that $k > k_c(R)$.

Appendix I Proof of Proposition 1

Assume that the solution is not unique, and there exists a second (or more) pair of solutions $N_v = \hat{N}_v$ and $N_b = \hat{N}_b$ under the current pair of decision variables (R, k), such that the equilibrium conditions in Equation (23) are satisfied and this pair of solutions causes the system to lie in one of three scenarios: RP-SD, WP-SD, or DD. Additionally, the first pair of solutions causes the system to lie in one of the three scenarios. Without loss of generality, we assume the system is under the RP-SD scenario for the first pair of solutions. Then, the second pair of solutions must not cause the system to lie in the RP-SD scenario, because we have already shown that there is only one valid solution for the RP-SD scenario. Thus, the system is under either the WP-SD scenario or the DD scenario. However, since both $\mathcal{L}_{RP,WP}$ and $\mathcal{L}_{SD,DD}$ are only dependent on the decision variables under certain given exogenous variables, the current decision variables (R, k) cannot cause the system to line in a scenario other than the RP-SD scenario, which yields a contradiction. Therefore, the second pair of solutions $(\hat{N}_b, \hat{N}_v)$ does not exist and the solution (N_b, N_v) under each pair of decision variables (R, k) is unique. Since the system equilibrium solution exists and is unique for each pair of decision variables (R, k), the regions of all three scenarios are mutually exclusive in $\mathcal{S}$ in the R-k coordinate system.

Appendix J Proof of Table 2

J.1 Properties of N_v

For $\delta = \overline{q}/R_a^2$, we have

$$N_v = N - \frac{6R^3\overline{q} - 3R^2\overline{q}\tau v + 2\sqrt{2\pi R_a^2 M R^3 \overline{q} k^2 v + 9R^6\overline{q}^2}}{6R_a^2 kv}. \tag{68}$$

Consider the derivatives

$$\frac{\mathrm{d}N_v}{\mathrm{d}R} = -\frac{R\overline{q}\left(\pi R_a^2 M R k^2 v + 9R^4\overline{q} + (3R - \tau v)\sqrt{2\pi R_a^2 M R^3 \overline{q} k^2 v + 9R^6\overline{q}^2}\right)}{R_a^2 kv\sqrt{R^3\overline{q}\left(2\pi R_a^2 M k^2 v + 9R^3\overline{q}\right)}}, \tag{69}$$

$$\frac{\mathrm{d}N_v}{\mathrm{d}k} = \frac{R^2\overline{q}\left(6R^4\overline{q} + (2R - \tau v)\sqrt{2\pi R_a^2 M R^3 \overline{q} k^2 v + 9R^6\overline{q}^2}\right)}{2R_a^2 k^2 v\sqrt{R^3\overline{q}\left(2\pi R_a^2 M k^2 v + 9R^3\overline{q}\right)}} > 0. \tag{70}$$

Since it is assumed that $R > \tau v$. Thus, N_v decreases with R and increases with k.

J.2 Properties of N_b, W_p, $W_{c,q}$, $W_{v,q}$, λ, W_v

Recall from Equation (29) that $N_b = \lambda\tau = \frac{R^2\overline{q}\tau}{R_a^2 k}$. It is straightforward that, N_b monotonically decreases with k, while it monotonically increases with R.

Recall from Equation (11) and Equation (13) that $W_p = 2R/(kv)$, which increases with R and decreases with k.

Recall from Equation (5) that $W_{c,q} = \tau/2$, which is straightforward that $W_{c,q}$ is not impacted by R or k.

Recall from Equation (6) that

$$W_{v,q} = \frac{\tau N_v}{N_b} - \frac{\tau}{2} = \frac{N_v}{\lambda} - \frac{\tau}{2} \tag{71}$$

$$= \frac{R_a^2 N k}{R^2 \overline{q}} - \frac{R}{v} - \frac{\sqrt{2\pi R_a^2 M R^3 \overline{q} k^2 v + 9R^6 \overline{q}^2}}{3R^2 \overline{q} v}. \tag{72}$$

$W_{v,q}$ decreases with R because N_v decreases with R and λ increases with R. $W_{v,q}$ increases with k because N_v increases with k and λ decreases with k.

Recall that in equilibrium, $\lambda = q/k = \overline{q}R^2/(R_a^2 k)$. Therefore, λ increases with R, and decreases with k.

Recall that according to vehicle conservation, $W_v = N/\lambda$. Therefore, W_v increases with k and decreases with R.

J.3 Properties of $W_{v,d}$

From equilibrium condition Equation (23b) we have

$$W_{v,d} = \frac{N - N_v}{\lambda} - W_p + \frac{\tau}{2} = \frac{3R^3\overline{q}k - 6R^3\overline{q} + k\sqrt{2\pi R_a^2 M R^3 \overline{q} k^2 v + 9R^6 \overline{q}^2}}{3R^2 \overline{q} k v}, \tag{73}$$

$$\frac{\mathrm{d}W_{v,d}}{\mathrm{d}R} = -\frac{\pi R_a^2 M k^3 v - 9R^3\overline{q}k - 3k\sqrt{2\pi R_a^2 M R^3 \overline{q} k^2 v + 9R^6 \overline{q}^2} + 6\sqrt{2\pi R_a^2 M R^3 \overline{q} k^2 v + 9R^6 \overline{q}^2}}{3kv\sqrt{2\pi R_a^2 M R^3 \overline{q} k^2 v + 9R^6 \overline{q}^2}} = 0, \tag{74}$$

$$\Longrightarrow R = \frac{\pi R_a^2 M k^2 v \left(k^2 - 2k + 2 - (k-2)\sqrt{k^2 - k + 1}\right)}{18\overline{q}(k-1)}. \tag{75}$$

The second-order derivative of $W_{v,d}$ with respect to R indicates that there exists a minimum value because

$$\frac{\mathrm{d}^2}{\mathrm{d}R^2} W_{v,d} = \frac{\pi R_a^2 M k^2 \left(\pi R_a^2 M k^2 v + 18R^3\overline{q}\right)}{R\sqrt{2\pi R_a^2 M R^3 \overline{q} v + 9R^6 \overline{q}^2}\left(2\pi R_a^2 M k^2 v + 9R^3\overline{q}\right)} > 0. \tag{76}$$

Therefore, $W_{v,d}$ first increase, then decrease, then increase.

$$\frac{\mathrm{d}W_{v,d}}{\mathrm{d}k} = \frac{2R\left(\pi R_a^2 M k^3 v + 3\sqrt{2\pi R_a^2 M R^3 \overline{q} k^2 v + 9R^6 \overline{q}^2}\right)}{3k^2 v\sqrt{2\pi R_a^2 M R^3 \overline{q} v + 9R^6 \overline{q}^2}} > 0. \tag{77}$$

Thus, $W_{v,d}$ increases with k.

J.4 Properties of $W_{c,d}$

Recall from Equation (15) that when $\theta = M\pi/(N - N_v)$

$$W_{c,d} = \frac{L_d + L_p}{2v} = \frac{9R + \dfrac{kRM\pi}{N - N_v}}{9v}. \tag{78}$$

Consider derivatives:

$$\frac{\mathrm{d}W_{c,d}}{\mathrm{d}R} = -\frac{\pi R_a^2 M k^2 v - 9R^3\overline{q} - 3\sqrt{2\pi R_a^2 M R^3 \overline{q} k^2 v + 9R^6 \overline{q}^2}}{6v\sqrt{2\pi R_a^2 M R^3 \overline{q} k^2 v + 9R^6 \overline{q}^2}}, \tag{79}$$

where the critical R is $R_c = \sqrt[3]{\dfrac{\pi R_a^2 M k^2 v}{36\overline{q}}}$ which increases with k and $\overline{q}$.

$$\frac{\mathrm{d}W_{c,d}}{\mathrm{d}k} = \frac{\pi R_a^2 M R k}{3\sqrt{2\pi R_a^2 M R^3 \overline{q} k^2 v + 9R^6 \overline{q}^2}} > 0. \tag{80}$$

For R, when $R \to \infty$, $\mathrm{d}W_{c,d}/\mathrm{d}R = \overline{q}/(v\overline{q}) > 0$. When $R \to 0^+$, $\mathrm{d}W_{c,d}/\mathrm{d}R \to -\infty$. Therefore, $W_{c,d}$ first decreases then increases with R. Through other derivatives, it can be known that $W_{c,d}$ increases with k.

J.5 Properties of $W_{c,a}$

Recall from Equation (4) that $W_{c,a} = \frac{k-1}{2\left(q/\overline{N}_w\right)}$ where $\overline{N}_w = N - N_v + \lambda\tau/2$ (see Equation (28)), and thus

$$W_{c,a} = \frac{(k-1)\left(3R^3\overline{q} + \sqrt{2\pi MR^3R_a^2\overline{q}k^2v + 9R^6\overline{q}^2}\right)}{6R^2\overline{q}kv}. \tag{81}$$

Consider derivatives:

$$\frac{\mathrm{d}W_{c,a}}{\mathrm{d}R} = -\frac{(k-1)\left(\pi MR_a^2k^2v - 9R^3\overline{q} - 3\sqrt{2\pi MR^3R_a^2\overline{q}k^2v + 9R^6\overline{q}^2}\right)}{6kv\sqrt{R^3\overline{q}\left(2\pi MR_a^2k^2v + 9R^3\overline{q}\right)}}, \tag{82}$$

which is negative when $\pi MR_a^2k^2v > 9R^3\overline{q} + 3\sqrt{2\pi MR^3R_a^2\overline{q}k^2v + 9R^6\overline{q}^2}$ (e.g., large R or large $\overline{q}$, etc.) and non-negative otherwise, and it shows that $W_{c,a}$ first decreases and then increases with R.

$$\frac{\mathrm{d}W_{c,a}}{\mathrm{d}k} = \frac{R\left(2\pi MR_a^2k^3v + 9R^3\overline{q} + 3\sqrt{2\pi MR^3R_a^2\overline{q}k^2v + 9R^6\overline{q}^2}\right)}{6k^2v\sqrt{R^3\overline{q}\left(2\pi MR_a^2k^2v + 9R^3\overline{q}\right)}} > 0, \tag{83}$$

which indicates that $W_{c,a}$ increases with k.

J.6 Properties of W_c

The customer total waiting time is the summation of all customer waiting times, i.e., $W_c = W_{c,q} + W_{c,d} + W_p + W_{c,a}$. Consider derivatives

$$\frac{\mathrm{d}W_c}{\mathrm{d}R} = -\frac{\pi MR_a^2k^2(2k-1)v - 9R^3\overline{q}(2k-1) - 3(2k+3)\sqrt{2\pi MR^3R_a^2\overline{q}k^2v + 9R^6\overline{q}^2}}{6kv\sqrt{R^3\overline{q}\left(2\pi MR_a^2k^2v + 9R^3\overline{q}\right)}}, \tag{84}$$

which is negative when R is small and non-negative when R is large, and it indicates that W_c first decreases and then increases with R.

$$\frac{\mathrm{d}W_c}{\mathrm{d}k} = \frac{R\left(4\pi MR_a^2k^3v + 9R^3\overline{q} - 9\sqrt{2\pi MR^3R_a^2\overline{q}k^2v + 9R^6\overline{q}^2}\right)}{6k^2v\sqrt{R^3\overline{q}\left(2\pi MR_a^2k^2v + 9R^3\overline{q}\right)}}, \tag{85}$$

which is non-negative when R is small (i.e., the included customer demand is low) such that $4\pi MR_a^2k^3v \geq -9R^3\overline{q} + 9\sqrt{2\pi MR^3R_a^2\overline{q}k^2v + 9R^6\overline{q}^2}$, and it is first non-negative and then negative when R is large.

Appendix K Proof of Table 3

K.1 Properties of N_v

Recall from Equation (30) that when $R_s = R + W_{fp}v/2 = R - R/k - \tau v/4 + v\tau_M/2$ and $q = \overline{q}R^2/R_a^2$,

$$N_v = N - \frac{3R^2\overline{q}(2R_s - \tau v) + 2\sqrt{2\pi R_a^2MR^3\overline{q}k^2v + 9R^4R_s^2\overline{q}^2}}{6R_a^2kv}. \tag{86}$$

$R_s = R + W_{fp}v/2 > R$, thus $2R_s > \tau v$. Also, $\mathrm{d}R_s/\mathrm{d}R = 1 - 1/k > 0$, N_v decreases with R.

$$\frac{\mathrm{d}N_v}{\mathrm{d}k} = \frac{-\frac{R^3\overline{q}}{k} - \frac{\frac{2\pi R_a^2MR^3\overline{q}k^2v}{9} + \frac{R^5\overline{q}^2R_s}{k}}{\sqrt{\frac{2\pi R_a^2MR^3\overline{q}k^2v}{9} + R^4\overline{q}^2R_s^2}} - \frac{R^2\overline{q}\tau v}{2} + R^2\overline{q}R_s + \sqrt{\frac{2\pi R_a^2MR^3\overline{q}k^2v}{9} + R^4\overline{q}^2R_s^2}}{R_a^2k^2v} \tag{87}$$

$$= \frac{R^2\overline{q}\left(-\frac{R}{k} - \frac{\frac{2\pi R_a^2 M k^2 v}{9R\overline{q}} + \frac{RR_s}{k}}{\sqrt{\frac{2\pi R_a^2 M k^2 v}{9R\overline{q}} + R_s^2}} - \frac{\tau v}{2} + R_s + \sqrt{\frac{2\pi R_a^2 M k^2 v}{9R\overline{q}} + R_s^2}\right)}{R_a^2 k^2 v}. \tag{88}$$

Since $R_s > R$, $R_s - \frac{R}{k} - \frac{\tau v}{2} > R - \frac{R}{k} - \frac{\tau v}{2} > 0$. Also, $\sqrt{\frac{2\pi R_a^2 M k^2 v}{9R\overline{q}} + R_s^2} - \frac{\frac{2\pi R_a^2 M k^2 v}{9R\overline{q}} + \frac{RR_s}{k}}{\sqrt{\frac{2\pi R_a^2 M k^2 v}{9R\overline{q}} + R_s^2}} > \sqrt{\frac{2\pi R_a^2 M k^2 v}{9R\overline{q}} + R_s^2} - \frac{\frac{2\pi R_a^2 M k^2 v}{9R\overline{q}} + \frac{RR_s}{k}}{\sqrt{\frac{2\pi R_a^2 M k^2 v}{9R\overline{q}} + \frac{RR_s}{k}}} > 0$ because $R_s^2 > \frac{RR_s}{k}$. Thus, $\frac{\partial N_v}{\partial k} > 0$, which indicates that N_v increases with k.

K.2 Properties of N_b, W_p, $W_{c,q}$, $W_{c,a}$, $W_{v,q}$, λ, W_v

Their properties are the same as those of the scenario when $W_{fp} = 0$ by the same logic.

K.3 Properties of $W_{c,d}$

Recall from Equation (15) that

$$\begin{aligned} W_{c,d} &= \frac{L_d + L_p}{2v} \\ &= \frac{W_{v,d} + W_p}{2}, \end{aligned} \tag{89}$$

where $W_{v,d} = \frac{N - N_v}{\lambda} - W_p - W_{fp} + \frac{\tau}{2}$. If we consider $W_{c,d}$ as a function of R and R_s and R_s as a function of R, we have

$$\frac{\mathrm{d}W_{c,d}(R)}{\mathrm{d}R} = \frac{\partial W_{c,d}(R,R_s)}{\partial R} + \frac{\partial W_{c,d}(R,R_s)}{\partial R_s}\frac{\mathrm{d}R_s(R)}{\mathrm{d}R} \tag{90}$$

$$= \frac{-\pi R_a^2 M k^3 v + 6\sqrt{2\pi R_a^2 M R^3 \overline{q} k^2 v + 9R^4 R_s^2 \overline{q}^2}}{6kv\sqrt{2\pi R_a^2 M R^3 \overline{q} k^2 v + 9R^4 R_s^2 \overline{q}^2}} + \frac{(k-1)\left(3R^2 R_s \overline{q} + \sqrt{2\pi R_a^2 M R^3 \overline{q} k^2 v + 9R^4 R_s^2 \overline{q}^2}\right)}{2kv\sqrt{2\pi R_a^2 M R^3 \overline{q} k^2 v + 9R^4 R_s^2 \overline{q}^2}} \tag{91}$$

$$= \frac{-\pi R_a^2 M k^3 v + 9R^2 R_s \overline{q}(k-1) + 3(k+1)\sqrt{2\pi R_a^2 M R^3 \overline{q} k^2 v + 9R^4 R_s^2 \overline{q}^2}}{6kv\sqrt{2\pi R_a^2 M R^3 \overline{q} k^2 v + 9R^4 R_s^2 \overline{q}^2}}. \tag{92}$$

The numerator is an increasing function of R. When $R \to 0^+$, $\frac{\mathrm{d}W_{c,d}}{\mathrm{d}R} \to -\infty$ and when $R \to \infty$, $\frac{\mathrm{d}W_{c,d}}{\mathrm{d}R} \to \frac{1}{v} > 0$. Therefore, $W_{c,d}$ first decreases then increases with R.

Similar to R, consider $W_{c,d}$ as a function of k and R_s and R_s as a function of k,

$$\frac{\mathrm{d}W_{c,d}(k)}{\mathrm{d}k} = \frac{\partial W_{c,d}(k,R_s)}{\partial k} + \frac{\partial W_{c,d}(k,R_s)}{\partial R_s}\frac{\mathrm{d}R_s(k)}{\mathrm{d}k} \tag{93}$$

$$= \frac{\pi R_a^2 M R k^3 v - 3R\sqrt{2\pi R_a^2 M R^3 \overline{q} k^2 v + 9R^4 R_s^2 \overline{q}^2}}{3k^2 v\sqrt{2\pi R_a^2 M R^3 \overline{q} k^2 v + 9R^4 R_s^2 \overline{q}^2}} + \frac{3R^3 R_s \overline{q} + R\sqrt{2\pi R_a^2 M R^3 \overline{q} k^2 v + 9R^4 R_s^2 \overline{q}^2}}{2k^2 v\sqrt{2\pi R_a^2 M R^3 \overline{q} k^2 v + 9R^4 R_s^2 \overline{q}^2}} \tag{94}$$

$$= \frac{R\left(2\pi R_a^2 M k^3 v + 9R^2 R_s \overline{q} - 3\sqrt{2\pi R_a^2 M R^3 \overline{q} k^2 v + 9R^4 R_s^2 \overline{q}^2}\right)}{6k^2 v\sqrt{2\pi R_a^2 M R^3 \overline{q} k^2 v + 9R^4 R_s^2 \overline{q}^2}}, \tag{95}$$

which is greater than 0 when $k \geq 2$. Therefore, $W_{c,d}$ increases with k.

K.4 Properties of $W_{v,d}$

Recall from Equation (12) that $W_{v,d} = 2R(1+k\theta/9-1/k)/v = 2W_{c,d} - W_p$. Then, $W_{v,d}$ increases with k.

For R, since $W_{v,d} = 2W_{c,d} - W_p$, $\partial W_{v,d}/\partial R = 2\partial W_{c,d}/\partial R - 2/(kv)$. Similar to the scenario for $W_{c,d}$, there exists a zero point of the derivative.

K.5 Properties of W_{fp}

$W_{fp} = -\dfrac{2R}{kv} - \dfrac{\tau}{2} + \tau_M$, which decreases with R and increases with k.

K.6 Properties of $W_{c,a}$

Recall from Equation (4) that $W_{c,a} = \frac{k-1}{2\left(q/\overline{N}_w\right)}$ where $\overline{N}_w = N - N_v + \lambda\tau/2$ (see Equation (30)). Let $R_s = R + W_s v/2$, we have

$$W_{c,a} = \frac{(k-1)\left(3R^2 R_s\overline{q} + \sqrt{2\pi M R^3 R_a^2\overline{q}k^2 v + 9R^4 R_s^2\overline{q}^2}\right)}{6R^2\overline{q}kv}. \tag{96}$$

Consider derivatives:

$$\frac{\mathrm{d}W_{c,a}}{\mathrm{d}R} = -\frac{(k-1)\left(\pi R_a^2 Mk^3 v - 9(k-1)R^2 R_s\overline{q} - 3(k-1)\sqrt{2\pi R_a^2 MR^3\overline{q}k^2 v + 9R^4 R_s^2\overline{q}^2}\right)}{6k^2 v\sqrt{R^3\overline{q}\left(2\pi R_a^2 Mk^2 v + 9RR_s^2\overline{q}\right)}}, \tag{97}$$

which is negative when $\pi R_a^2 Mk^3 v - 9(k-1)R^2 R_s\overline{q} - 3(k-1)\sqrt{2\pi R_a^2 MR^3\overline{q}k^2 v + 9R^4 R_s^2\overline{q}^2}$ (e.g., large R or large $\overline{q}$, etc.) and non-negative otherwise, and it shows that $W_{c,a}$ first decreases and then increases with R.

$$\frac{\mathrm{d}W_{c,a}}{\mathrm{d}k} = \frac{2\pi R_a^2 MRk^4 v + 9R^2 R_s\overline{q}(Rk - R + R_s k) + (3Rk - 3R + 3R_s k)\sqrt{2\pi R_a^2 MR^3\overline{q}k^2 v + 9R^4 R_s^2\overline{q}^2}}{12k^3 v\sqrt{R^3\overline{q}\left(2\pi R_a^2 Mk^2 v + 9RR_s^2\overline{q}\right)}} > 0, \tag{98}$$

which indicates that $W_{c,a}$ increases with k.

K.7 Properties of W_c

Consider derivatives

$$\frac{\mathrm{d}W_c}{\mathrm{d}R} = \frac{\partial W_c}{\partial R} + \frac{\partial W_c}{\partial R_s}\frac{\mathrm{d}R_s}{\mathrm{d}R} \tag{99}$$

$$= -\frac{\pi R_a^2 Mk^3(2k-1)v - 9R^2 R_s\overline{q}(2k-1)(k-1) - (6k^2 - 3k + 3)\sqrt{2\pi R_a^2 MR^3\overline{q}k^2 v + 9R^4 R_s^2\overline{q}^2}}{6k^2 v\sqrt{R^3\overline{q}\left(2\pi R_a^2 Mk^2 v + 9RR_s^2\overline{q}\right)}}, \tag{100}$$

which is negative when R is small such that $\pi R_a^2 Mk^3(2k-1)v > 9R^2 R_s\overline{q}(2k-1)(k-1) + (6k^2 - 3k + 3)\sqrt{2\pi R_a^2 MR^3\overline{q}k^2 v + 9R^4 R_s^2\overline{q}^2}$ and non-negative otherwise. Therefore, W_c first decreases and then increases with R.

$$\frac{\mathrm{d}W_c}{\mathrm{d}k} = \frac{\partial W_c}{\partial k} + \frac{\partial W_c}{\partial R_s}\frac{\mathrm{d}R_s}{\mathrm{d}k} \tag{101}$$

$$= \frac{4\pi R_a^2 MRk^4 v + 18R^3 R_s\overline{q}k + 9R^2 R_s^2\overline{q}(k-1) + (3R_s k - 3R)\sqrt{2\pi R_a^2 MR^3\overline{q}k^2 v + 9R^4 R_s^2\overline{q}^2}}{6k^3 v\sqrt{R^3\overline{q}\left(2\pi R_a^2 Mk^2 v + 9RR_s^2\overline{q}\right)}} > 0, \tag{102}$$

which shows that W_c increases with k.

Appendix L Proof of Table 4

L.1 Properties of N_b

$$N_b = \frac{4\pi MR^3 k\overline{q}}{18R_a^2 Nkv - 9R^2\overline{q}\tau v} + \frac{R^2\overline{q}\tau_M}{R_a^2 k} + \frac{2R^3\overline{q}}{R_a^2 kv} - \frac{2R^3\overline{q}}{R_a^2 k^2 v} + \frac{R^2\overline{q}\tau}{R_a^2 k} - N \tag{103}$$

$$= \frac{4\pi MRk\lambda}{9v(2N-\lambda\tau)} - N + \frac{2R\lambda}{v} - \frac{2R\lambda}{kv} + \lambda\tau + \lambda\tau_M \tag{104}$$

$$= \frac{4\pi MRk}{9v(2N/\lambda-\tau)} - N + \frac{2R\lambda}{v}\left(1-\frac{1}{k}\right) + \lambda\tau + \lambda\tau_M, \tag{105}$$

which increases with R and decreases with k, since $k \geq 2$.

L.2 Properties of $W_{v,d}$

$$W_{v,d} = \frac{N-N_v}{\lambda} - W_p - W_{fp} + \frac{\tau}{2}, \tag{106}$$

$$\frac{\mathrm{d}W_{v,d}}{\mathrm{d}R} = \frac{8\pi R_a^4 MNk^4 + 4\pi R_a^2 MR^2\overline{q}k^3\tau + 18R^4\overline{q}^2\tau^2(k-1) + 72R_a^2 Nk(k-1)(R_a^2 Nk - R^2\overline{q}\tau)}{9kv\left(2R_a^2 Nk - R^2\overline{q}\tau\right)^2} > 0, \tag{107}$$

$$\frac{\mathrm{d}W_{v,d}}{\mathrm{d}k} = \frac{2R\left(4\pi R_a^4 MNk^4 + 36R_a^4 N^2k^2 - 4\pi R_a^2 MR^2\overline{q}k^3\tau - 36R_a^2 NR^2\overline{q}k\tau + 9R^4\overline{q}^2\tau^2\right)}{9k^2 v\left(2R_a^2 Nk - R^2\overline{q}\tau\right)^2} > 0. \tag{108}$$

L.3 Properties of $W_{c,d}$

$$W_{v,d} = \frac{N-N_v}{\lambda} - W_p - W_{fp} + \frac{\tau}{2}, \tag{109}$$

$$W_{c,d} = \frac{W_{v,d} + W_p}{2}. \tag{110}$$

Since $N > N_v = \lambda\tau$, $R_a^2 Nk > R^2\overline{q}\tau$, then we have

$$\frac{\mathrm{d}W_{c,d}}{\mathrm{d}R} = \frac{4\pi R_a^4 MNk^3 + 36R_a^4 N^2k^2 + 2\pi R_a^2 MR^2\overline{q}k^2\tau - 36R_a^2 NR^2\overline{q}k\tau + 9R^4\overline{q}^2\tau^2}{9v\left(2R_a^2 Nk - R^2\overline{q}\tau\right)^2} > 0, \tag{111}$$

$$\frac{\mathrm{d}W_{c,d}}{\mathrm{d}k} = \frac{4\pi R_a^2 MRk\left(R_a^2 Nk - R^2\overline{q}\tau\right)}{9v\left(2R_a^2 Nk - R^2\overline{q}\tau\right)^2} > 0. \tag{112}$$

L.4 Properties of W_{fp}

$$W_{fp} = \tau_M - W_{c,q} - W_p \tag{113}$$

$$= -\frac{4\pi MRk}{18Nv - 9\dfrac{\overline{q}R^2}{R_a^2 k}\tau v} + \frac{N}{\lambda} - \frac{2R}{v} - \frac{\tau}{2}, \tag{114}$$

which decreases with R.

$$\frac{\mathrm{d}W_{fp}}{\mathrm{d}k} = \frac{R_a^2\left(36R_a^4 N^3k^2v - 8\pi R_a^2 MNR^3\overline{q}k^2 - 36R_a^2 N^2R^2\overline{q}k\tau v + 8\pi MR^5\overline{q}^2k\tau + 9NR^4\overline{q}^2\tau^2 v\right)}{9R^2\overline{q}v\left(2R_a^2 Nk - R^2\overline{q}\tau\right)^2} \tag{115}$$

$$= \frac{R_a^2\left[(36R_a^2 N^2kv - 8\pi MR^3\overline{q}k)(R_a^2 Nk - R^2\overline{q}\tau) + 9NR^4\overline{q}^2\tau^2 v\right]}{9R^2\overline{q}v\left(2R_a^2 Nk - R^2\overline{q}\tau\right)^2}, \tag{116}$$

where $R_a^2Nk > R^2\overline{q}\tau$ because $N > \lambda\tau$. To compare $36R_a^2N^2kv$ and $8\pi MR^3\overline{q}k$, we compare the result of $36R_a^2N^2kv$ divided by $8\pi MR^3\overline{q}k$ with 1:

$$\frac{36R_a^2N^2kv}{8\pi MR^3\overline{q}k} = \frac{N\dfrac{N}{M}}{\dfrac{2\pi Rk}{9v}\dfrac{R^2\overline{q}}{R_a^2k}}, \tag{117}$$

which is greater than 1 because $N > M$, and the denominator represents the number of drivers who are transversely traveling, which is normally much smaller than the fleet size. Consequently, W_{fp} increases with k.

L.5 Properties of $W_{c,q}$

$$W_{c,q} = \frac{N_b\tau}{N_v} - \frac{\tau}{2} = \frac{N_b}{\lambda} - \frac{\tau}{2} \tag{118}$$

$$= \frac{4\pi MRk}{18Nv - 9\dfrac{\overline{q}R^2}{R_a^2k}\tau v} - \frac{N}{\lambda} + \frac{2R}{v} - \frac{2R}{kv} + \frac{\tau}{2} + \tau_M. \tag{119}$$

It is straightforward that $W_{c,q}$ increases with R. For k, consider the derivative:

$$\frac{\mathrm{d}W_{c,q}}{\mathrm{d}k} = -\frac{(9R_a^2N^2k^2v - 2\pi MR^3\overline{q}k^2 - 18NR^3\overline{q})(R_a^2Nk - R^2\overline{q}\tau)\cdot 4R_a^2k + 9R_a^2NR^4\overline{q}^2k^2\tau^2v - 18R^7\overline{q}^3\tau^2}{9R^2\overline{q}k^2v\left(2R_a^2Nk - R^2\overline{q}\tau\right)^2}. \tag{120}$$

This derivative is negative as follows. Since the number of drivers who are heading for pickup and delivery should be smaller than the vehicle fleet size, we have

$$N > \frac{2R}{v}\frac{\overline{q}R^2}{R_a^2k} + \frac{2\theta Rk}{9v}\frac{\overline{q}R^2}{R_a^2k}. \tag{121}$$

Then, multiply both sides with Nk^2

$$N^2k^2 > \frac{2R}{v}\frac{\overline{q}R^2}{R_a^2}Nk + \frac{2M\pi Rk}{9v}\frac{\overline{q}R^2}{R_a^2}\frac{N}{N - N_v + \frac{\lambda\tau}{2}}k \tag{122}$$

$$> \frac{2R}{v}\frac{\overline{q}R^2}{R_a^2}Nk + \frac{2\pi MRk}{9v}\frac{\overline{q}R^2}{R_a^2}k. \tag{123}$$

Simplify and we obtain

$$9R_a^2N^2k^2v > 18\overline{q}R^3Nk + 2\pi M\overline{q}R^3k^2 > 18NR^3\overline{q} + 2\pi MR^3\overline{q}k^2, \tag{124}$$

which shows that the right-hand side is the term inside the first parenthesis of the numerator of Equation (120), $9R_a^2N^2k^2v - 2\pi MR^3\overline{q}k^2 - 18NR^3\overline{q}$ is greater than 0.

Second, $R_a^2Nk - R^2\overline{q}\tau > 0$ because $N > \lambda\tau$.

Third, $\dfrac{1}{q/M} \geq \tau_M > W_p = \dfrac{2R}{kv}$, then $R_a^2Mkv > 2R^3\overline{q}$, and $R_a^2Nk^2v > R_a^2Mkv > 2R^3\overline{q}$. Then we can get $9R_a^2NR^4\overline{q}^2k^2\tau^2v > 18R^7\overline{q}^3\tau^2$.

Finally, all the terms of the numerator of Equation (120) are greater than 0, and $\dfrac{\mathrm{d}W_{c,q}}{\mathrm{d}k}$ is therefore negative.

L.6 Properties of $W_{c,a}$

Consider derivatives

$$\frac{\mathrm{d}W_{c,a}}{\mathrm{d}R} = -\frac{NR_a^2(k-1)}{R^3\overline{q}} < 0, \tag{125}$$

$$\frac{\mathrm{d}W_{c,a}}{\mathrm{d}k} = \frac{2NR_a^2k^2 - R^2\overline{q}\tau}{4R^2\overline{q}k^2} > 0, \tag{126}$$

which shows that $W_{c,a}$ decreases with R and increases with k.

L.7 Properties of W_c

Since $W_{fp} = \tau_M - W_p - W_{cq}$, we have

$$W_c = W_{c,a} + W_{c,d} + \tau_M, \tag{127}$$

$$\frac{\mathrm{d}W_c}{\mathrm{d}R} = -\frac{R_a^2 M(k-1)}{R^3\overline{q}} + \frac{4\pi R_a^4 MNk^3 + 36R_a^4N^2k^2 + 2\pi R_a^2 MR^2\overline{q}k^2\tau - 36R_a^2NR^2\overline{q}k\tau + 9R^4\overline{q}^2\tau^2}{9v\left(2R_a^2Nk - R^2\overline{q}\tau\right)^2}, \tag{128}$$

which approaches $-\infty$ when $R \to 0^+$ and approaches $1/v > 0$ when $R \to \infty$. Also, on the boundary condition $\mathcal{L}_{SD,DD}$, we have $\frac{\mathrm{d}W_c}{\mathrm{d}R} = -\frac{2NR_a^2k^2v - NR_a^2kv - R^3\overline{q}}{R^3\overline{q}kv} < 0$, and on $\mathcal{L}_e$, we have $\frac{\mathrm{d}W_c}{\mathrm{d}R} = -\frac{2NR_a^2k^2v - NR_a^2kv - 2R^3\overline{q}}{R^3\overline{q}kv} < 0$. Thus, W_c decreases with R.

$$\frac{\mathrm{d}W_c}{\mathrm{d}k} = \frac{\begin{array}{c}16\pi MR^3R_a^2\overline{q}k^3(NkR_a^2 - \overline{q}\tau R^2) + 36N^2R_a^4k^2v(2Nk^2R_a^2 - 2\overline{q}k\tau R^2 - \overline{q}\tau R^2)\\ +18NR^4R_a^2\overline{q}^2k(k+2)\tau^2v - 9R^6\overline{q}^3\tau^3v\end{array}}{36R^2\overline{q}k^2v\left(2NR_a^2k - R^2\overline{q}\tau\right)^2} > 0, \tag{129}$$

which shows that W_c increases with k.

Appendix M Proof of part of Proposition 3

In the WP-DD scenario, k increases customer total waiting time, and thus a small k is featured. For the delivery radius, we first look at accumulation time $W_{c,a}$ and customers' delivery time $W_{c,d}$ because $W_c = \tau_M + W_{c,a} + W_{c,d}$. On the boundary $\mathcal{L}_e$ we have

$$k_c = \frac{3R^2\overline{q}\left(6R_aNR + 3R_aN\tau v + \sqrt{2}R\sqrt{18R_a^2N^2 + 4\pi MR^2\overline{q}\tau + \pi MR\overline{q}\tau^2 v}\right)}{2R_a\left(9R_a^2N^2v - 2\pi MR^3\overline{q}\right)}. \tag{130}$$

We know from Equation (4) that $W_{c,a} = \frac{k-1}{2\left(q/\overline{N}_w\right)}$. Since we assume homogeneous demand for all merchants, it can also be written as

$$W_{c,a} = \frac{k-1}{2\left(q_{\text{sector}}\right)} = \frac{k-1}{2\left(q_{\text{single merchant}}/N_{\text{sectors}}\right)} = \frac{k-1}{2\left(q/M/(\pi/\theta)\right)}. \tag{131}$$

Substituting $k = k_c$ into the above equation, we have $W_{c,a} = W_{c,a}(R)$ meaning that $W_{c,a}$ is a function of R on the curve $\mathcal{L}_e$. Since k_c increases with R according to Lemma 1, to prove $W_{c,a}(R)$ increases with R, we then prove q_{sector} decreases with R. Consider derivatives

$$\frac{\mathrm{d}q_{\text{sector}}}{\mathrm{d}R} = -\frac{\begin{array}{c}3\overline{q}\left(8R+\tau v\right)\left(\begin{array}{c}324\sqrt{2}\Delta^4N^4 + 72\sqrt{2}\pi\Delta^2MN^2R^2\overline{q}\tau\\ +9\sqrt{2}\pi\Delta^2MN^2R\overline{q}\tau^2v + 2\sqrt{2}\pi^2M^2R^4\overline{q}^2\tau^2\\ +\left(-108\Delta^3N^3 - 12\pi\Delta MNR^2\overline{q}\tau\right)\sqrt{18\Delta^2N^2 + 4\pi MR^2\overline{q}\tau + \pi MR\overline{q}\tau^2v}\end{array}\right)\end{array}}{\begin{array}{c}2\Delta\left(18\Delta^2N^2 - 3\sqrt{2}\Delta N\sqrt{18\Delta^2N^2 + 4\pi MR^2\overline{q}\tau + \pi MR\overline{q}\tau^2v} + 2\pi MR^2\overline{q}\tau\right)^2\\ \cdot\sqrt{18\Delta^2N^2 + 4\pi MR^2\overline{q}\tau + \pi MR\overline{q}\tau^2v}\end{array}}. \tag{132}$$

We look into the numerator:

$$\begin{aligned}\text{numerator} =& 324\sqrt{2}\Delta^4N^4 + 72\sqrt{2}\pi\Delta^2MN^2R^2\overline{q}\tau + 9\sqrt{2}\pi\Delta^2MN^2R\overline{q}\tau^2v + 2\sqrt{2}\pi^2M^2R^4\overline{q}^2\tau^2\\ &+\left(-108\Delta^3N^3 - 12\pi\Delta MNR^2\overline{q}\tau\right)\sqrt{18\Delta^2N^2 + 4\pi MR^2\overline{q}\tau + \pi MR\overline{q}\tau^2v}.\end{aligned} \tag{133}$$

Let exp_A be the first line of the above expression and exp_B be the second line, since $exp_A^2 - exp_B^2 = 2\pi^2M^2R^2\overline{q}^2\tau^4\left(9\Delta^2N^2v - 2\pi MR^3\overline{q}\right)^2 > 0$, we have the numerator of Equation (132) is greater than 0 and thus $\frac{\mathrm{d}q_{\text{sector}}}{\mathrm{d}R} < 0$.

Then, we have $\frac{W_{c,a}(R)}{\mathrm{d}R} > 0$, which means that to seek smaller W_c, one should move toward the bottom-left direction (reduce R and meanwhile reduce k) along with $\mathcal{L}_e$ the $R-k$ coordinate system.

Appendix N Proof of Proposition 4

The formulation of q_t is shown as follows:

$$q_t = \begin{cases} q, & \text{stable system,} \\ \hat{q} = \dfrac{2Rk\left(2\pi Mk + 18N + 9N\tau v/R - 2\Delta_q\right)}{9\tau\left(4R+\tau v\right)}, & \text{unstable system,} \end{cases} \tag{134}$$

where $\Delta_q = \sqrt{\pi^2M^2k^2 + 18\pi MNk + 9\pi MNk\tau v/R + 81N^2}$, and q_t in an unstable system is solved by the critical condition $N_v = \lambda\tau$ and $W_{fp} = 0$.

We first discover the relationship between q_t and R. Rearranging Equation (36), we obtain

$$q_t = \frac{2k\left(2R\pi Mk + 18RN + 9N\tau v - 2\sqrt{\pi^2M^2k^2R^2 + 18\pi MNkR^2 + 9\pi MNk\tau vR + 81N^2R^2}\right)}{9\tau\left(4R+\tau v\right)} \tag{135}$$

$$= \frac{2k\left(2R(\pi Mk - 9N) + 9N(4R+\tau v) - 2\sqrt{(\pi Mk - 9N)^2R^2 + 9\pi MNkR(4R+\tau v)}\right)}{9\tau\left(4R+\tau v\right)} \tag{136}$$

$$= 2k\left(2\frac{R}{4R+\tau v}\frac{\pi Mk - 9N}{9\tau} + \frac{N}{\tau} - \frac{2}{\tau}\sqrt{\left(\frac{\pi Mk - 9N}{9}\right)^2\left(\frac{R}{4R+\tau v}\right)^2 + \frac{\pi MNk}{9}\frac{R}{4R+\tau v}}\right). \tag{137}$$

Denote two auxiliary variables $R_q = \dfrac{R}{4R+\tau v} \in \left[0, \dfrac{1}{4}\right)$ and $a = \dfrac{\pi Mk - 9N}{9}$. We have

$$q_t = \frac{2k}{\tau}\left(2aR_q + N - 2\sqrt{a^2R_q^2 + (a+N)NR_q}\right), \tag{138}$$

and its derivative with respect to R_q is

$$\frac{\partial q_t}{\partial R_q} = -\frac{2k\left(N^2 + Na + 2R_qa^2 - 2a\sqrt{N^2R_q + NR_qa + R_q^2a^2}\right)}{\tau\sqrt{N^2R_q + NR_qa + R_q^2a^2}}. \tag{139}$$

For $a < 0$,

$$\frac{\partial q_t}{\partial R_q} = -\frac{2k\left(N^2 + Na + 2R_qa^2 - 2a\sqrt{N^2R_q + NR_qa + R_q^2a^2}\right)}{\tau\sqrt{N^2R_q + NR_qa + R_q^2a^2}} \tag{140}$$

$$< -\frac{2k\left(N^2 + Na + 2R_qa^2 - 2a\sqrt{N^2R_q^2 + 2NR_q^2a + R_q^2a^2}\right)}{\tau\sqrt{N^2R_q + NR_qa + R_q^2a^2}} \tag{141}$$

$$= -\frac{2k\left[N(N+a) + 2R_qa^2 - 2aR_q(N+a)\right]}{\tau\sqrt{N^2R_q + NR_qa + R_q^2a^2}} < 0. \tag{142}$$

Therefore, $\partial q_t/R_q < 0$ for $a < 0$. For $a \geq 0$,

$$\frac{\partial q_t}{\partial R_q} = -\frac{2k\left(N^2 + Na + 2R_qa^2 - 2a\sqrt{N^2R_q + NR_qa + R_q^2a^2}\right)}{\tau\sqrt{N^2R_q + NR_qa + R_q^2a^2}} \tag{143}$$

$$< -\frac{2k\left(N^2 + Na + 2R_qa^2 - 2a\sqrt{N^2/4 + NR_qa + R_q^2a^2}\right)}{\tau\sqrt{N^2R_q + NR_qa + R_q^2a^2}} \tag{144}$$

$$= -\frac{2k\left[N^2 + Na + 2R_qa^2 - 2a(N/2 + R_qa)\right]}{\tau\sqrt{N^2R_q + NR_qa + R_q^2a^2}} \tag{145}$$

$$= -\frac{2kN^2}{\tau\sqrt{N^2R_q + NR_qa + R_q^2a^2}} < 0. \tag{146}$$

Therefore, $\partial q_t / R_q < 0$ for all a because $\dfrac{\mathrm{d}q_t}{\mathrm{d}R} = \dfrac{\partial q_t}{\partial R_q}\dfrac{\mathrm{d}R_q}{\mathrm{d}R}$, where $\dfrac{\mathrm{d}R_q}{\mathrm{d}R} > 0$.

For k, consider another auxiliary variable $k_q = a + N = \pi M k/9$. Then the derivative of Equation (138) with respect to k_q is

$$\frac{\partial q_t}{\partial k_q} = -\frac{18\left(2N^2R_q^2 - 6NR_q^2k_q + 3NR_qk_q + 4R_q^2k_q^2 + (2NR_q - N - 4R_qk_q)\sqrt{N^2R_q^2 - 2NR_q^2k_q + NR_qk_q + R_q^2k_q^2}\right)}{\pi M\tau\sqrt{N^2R_q^2 - 2NR_q^2k_q + NR_qk_q + R_q^2k_q^2}}. \tag{147}$$

The numerator is negative because if we denote $LHS = 2N^2R_q^2 - 6NR_q^2k_q + 3NR_qk_q + 4R_q^2k_q^2 > 0$ and $RHS = -(2NR_q - N - 4R_qk_q)\sqrt{N^2R_q^2 - 2NR_q^2k_q + NR_qk_q + R_q^2k_q^2}$, then $LHS^2 - RHS^2 = N^3R_q(4R_q - 1)(NR_q - 2R_qk_q + k_q) > 0$, which indicates that the numerator $= LHS - RHS > 0$. Therefore, the derivative of q_t with respect to k_q is greater than 0 and $\mathrm{d}q_t/\mathrm{d}k > 0$.